Chaotic braided solutions via rigorous numerics: chaos in the Swift-Hohenberg equation

Jan Bouwe van den Berg* Jean-Philippe Lessard†

Abstract

We prove that the stationary Swift-Hohenberg equation has chaotic dynamics on a critical energy level for a large (continuous) range of parameter values. The first step of the method relies on a computer assisted, rigorous, continuation method to prove the existence of a periodic orbit with certain geometric properties. The second step is topological: we use this periodic solution as a skeleton, through which we braid other solutions, thus forcing the existence of infinitely many braided periodic orbits. A semi-conjugacy to a subshift of finite type shows that the dynamics is chaotic.

1 Introduction

Finding analytic solutions of nonlinear, parameter dependent, ordinary differential equations (ODEs) is in general an extremely difficult task, most of the time impossible. The use of numerical techniques then becomes a useful path to adopt in order to understand the dynamics of a given nonlinear ODE. One may obtain insight not just through simulations, but nowadays the numerical output can also be used to rigorously extract coarse topological information from the systems, often revealing complicated dynamics. In particular, proving the existence of chaos in nonlinear dynamical systems in such a way has become quite popular (see [1, 13, 16, 24, 30, 32, 33]). One may interpret these results as forcing-type theorems, since a finite number of computable objects can be used to draw conclusions about the existence of infinitely many other objects. In this paper we propose a novel approach along those lines to prove existence of chaos for a class of problems with a special structure, namely so-called second-order Lagrangian dynamical systems with the Twist property. This is a class of variational problems that lead to fourth order ODEs. In particular, the well-known Swift-Hohenberg equation, one of standard models for pattern formation, falls into this class of problems.

A common feature of the proofs in [1, 16, 24, 32, 33] is the use of interval arithmetic to integrate the flow over sets and look for images of these rigorously integrated sets on some prescribed Poincaré sections. In contrast, our proof only requires proving the existence of *a single periodic solution* of a certain type. This will be done via validated continuation (cf. [14, 17]). One important advantage of this validated continuation

*VU University Amsterdam, Department of Mathematics, De Boelelaan 1081, 1081 HV Amsterdam, The Netherlands.

†Rutgers Univeristy, Department of Mathematics, Hill Center-Busch Campus, 110 Frelinghuysen Rd, Piscataway, NJ 08854-8019, USA. and VU University Amsterdam, Department of Mathematics, De Boelelaan 1081, 1081 HV Amsterdam, 1081 HV Amsterdam, The Netherlands.

method is that it becomes natural to prove the existence of chaos for a continuous range of parameter values.

We focus our attention on the Swift-Hohenberg equation, a fourth order parabolic partial differential equation (PDE), traditionally written as

$$\frac{\partial U}{\partial T} = -\left(\frac{\partial^2}{\partial X^2} + 1\right)^2 U + \alpha U - U^3, \tag{1}$$

which is widely used as a model for pattern formation due to a finite wavelength instability, such as in Rayleigh-Bénard convection (e.g., see [10, 29]). The onset of instability is at $\alpha = 0$. Stationary profiles satisfy the ODE

$$-U'''' - 2U'' + (\alpha - 1)U - U^3 = 0, \tag{2}$$

which has a constant of integration, called the *energy*

$$E = U'''U' - \frac{1}{2}U''^2 + U'^2 - \frac{\alpha - 1}{2}U^2 + \frac{1}{4}U^4 + \frac{(\alpha - 1)^2}{4},$$

which has been normalized so that, for $\alpha > 1$, the nontrivial homogeneous states $U = \pm\sqrt{\alpha - 1}$ have energy $E = 0$. The dynamics of (2) have been studied extensively, especially for small $\alpha > 0$, but many questions remain open for larger values of the parameter. Numerical simulations suggest chaotic behavior for most $\alpha > 0$, but this has so far not been verified rigorously. In particular, although both shooting methods (e.g. [2, 7, 8, 25]) and variational methods (e.g. [6, 20, 22, 27]) have been used extensively to study (2) and related fourth order equations, they have not succeeded in revealing chaos for the Swift-Hohenberg ODE.

The energy level $E = 0$ is special in the sense that it is a singular energy level, and it contains the nontrivial homogeneous states $U = \pm\sqrt{\alpha - 1}$. Those equilibria are stable solutions of the PDE (1) for $\alpha > \frac{3}{2}$, and saddle-foci for the ODE (2) in the same parameter range. It is well known that saddle-foci may act as organizing centers for complicated dynamics [15, 21], and this inspires us to focus our attention on the dynamics in the energy level $E = 0$. Our main result is to establish rigorously that the Swift-Hohenberg ODE has chaotic dynamics in the energy level $E = 0$ for a large continuous range of parameter values.

Proposition 1. *The dynamics of the Swift-Hohenberg ODE (2) on the energy level $E = 0$ is chaotic for all $\alpha \geq 2$.*

Before we discuss the method of proof, let us comment on some generalizations of this result. First, the method is amenable to a larger class of equations, namely second order Lagrangians with the Twist property, see [3]. Second, the result is stable in the sense that for energy levels arbitrarily close to 0, chaos can be proved via a few adjustments of the arguments. We will comment on both generalizations when appropriate, but keep the focus firmly on Proposition 1 to reduce technical details. Finally, the parameter range $\alpha \geq 2$ can be extended somewhat using our method, but certainly not to cover the entire range $\alpha > 0$, as will be explained below.

We now turn to the method behind Proposition 1. Rather than working directly with (2) we first perform a change of coordinates that compactifies the parameter range, as well as making the notation more convenient. The new variables are

$$y = \frac{X}{\sqrt[4]{\alpha - 1}}, \qquad u(y) = \frac{U(X)}{\sqrt{\alpha - 1}}, \qquad \nu = \frac{2}{\sqrt{\alpha - 1}}. \tag{3}$$

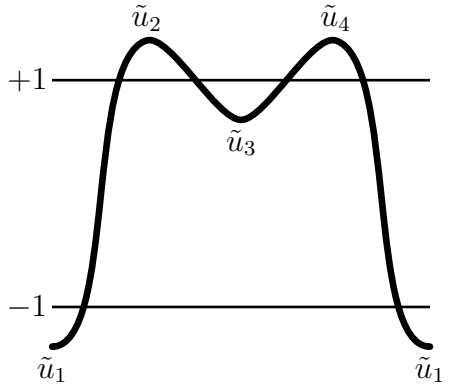

Figure 1: Sketch of a periodic solution $\widetilde{u}$ satisfying the geometric properties $\mathcal{H}$.

The parameter range $\alpha \geq 2$ corresponds to $\nu \in (0, 2]$, and the differential equation becomes

$$-u'''' - \nu u'' + u - u^3 = 0, \tag{4}$$

while the expression for the energy is now

$$E = u'''u' - \frac{1}{2}u''^2 + \frac{\nu}{2}u'^2 + \frac{1}{4}(u^2 - 1)^2. \tag{5}$$

Equation (4), and variants with different nonlinearities, have been thoroughly investigated (see [9] and [26] and the references therein), but the parameter range under scrutiny here, namely $\nu \geq 0$, remains much less explored than the range $\nu < 0$, mainly because most methods are somewhat less powerful for positive ν. An exception are the braid invariants introduced in [18], which are especially suited to deal with positive ν, and which we will indeed exploit in Section 2.

In the method presented in this paper, chaos is forced by the existence of a single periodic solution $\widetilde{u}$ with specific geometric properties, much like a period-3 solution of an interval map implies chaos [23] (or a pseudo-Anosov braid in the context of surface homeomorphisms [31]). The periodic solution we are looking for needs to satisfy the following geometric properties, see also Figure 1:

$$\mathcal{H} \begin{cases} (H_1) & \widetilde{u} \text{ has exactly four monotone laps and extrema } \{\widetilde{u}_i\}_{i=1}^4; \\ (H_2) & \widetilde{u}_1 \text{ and } \widetilde{u}_3 \text{ are minima, and } \widetilde{u}_2 \text{ and } \widetilde{u}_4 \text{ are maxima;} \\ (H_3) & \widetilde{u}_1 < -1 < \widetilde{u}_3 < 1 < \widetilde{u}_2, \widetilde{u}_4; \\ (H_4) & \widetilde{u} \text{ is symmetric in its minima } \widetilde{u}_1 \text{ and } \widetilde{u}_3. \end{cases}$$

Let the extrema $\widetilde{u}_i$ be attained in $\widetilde{y}_i$, then the last condition can be reformulated as

$$\widetilde{u}(\widetilde{y}_1 + y) = \widetilde{u}(\widetilde{y}_1 - y) \qquad \text{and} \qquad \widetilde{u}(\widetilde{y}_3 + y) = \widetilde{u}(\widetilde{y}_3 - y).$$

In particular, it implies that $\widetilde{u}_2 = \widetilde{u}_4$. We should note that condition H_4 is in fact not necessary for the results below to hold, but it simplifies the exposition.

As said before, such periodic solutions can be used to prove chaos when the equilibria $u = \pm 1$ are saddle-foci, i.e., when $\nu < \sqrt{8}$.

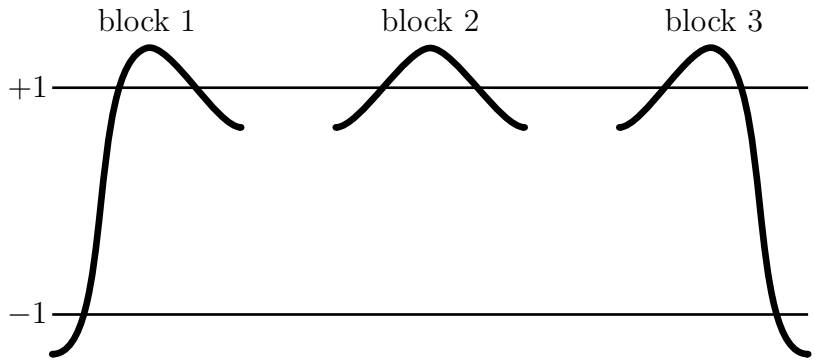

Figure 2: Building blocks for the solutions that lead to the chaos of Theorem 2.

Theorem 2 (forcing)**.** *Let $\nu \in [0, \sqrt{8})$, and suppose there exists a periodic solution $\widetilde{u}$ of (4) at the energy level $E = 0$, satisfying the geometric conditions $\mathcal{H}$. Then (4) is chaotic on the energy level $E = 0$ in the sense that there exists a two-dimensional Poincaré return map which has a compact invariant set on which the topological entropy is positive.*

The construction of the chaotic invariant set hinges on an application of Conley index theory for discretized braids [18], which will be adapted to our specific situation. The formulation in terms of discretized braids and the computation of the Conley index for well-chosen neighborhoods, whose construction involves the special periodic solution $\widetilde{u}$, is presented in Section 2, together with all details of the proof of Theorem 2. Let us briefly discuss some intuition behind the result. The set of solutions of (4) that leads us to chaotic dynamics is obtained by putting the three building blocks in Figure 2 together. The order of the blocks should follow the intuition coming from Figure 2, i.e., blocks 1 and 2 may be followed by block 2 or 3, while block 3 can only be followed by block 1. The sequence of building blocks may be chosen arbitrarily as long as these rules are obeyed, and the different possibilities are sufficiently complicated to lead to chaos. The final technical step in proving chaos is then to find a semi-conjugacy to a subshift of finite type, see Section 2.1.

It is important to note that the only hypothesis that needs to be verified in order to prove the existence of chaos in (4) at $E = 0$ is the existence of the periodic solution $\widetilde{u}$ satisfying $\mathcal{H}$. This will be done via rigorous numerics, or computer assisted (interval arithmetic) calculations, together with a set of analytic estimates of the "tail" terms, i.e., the remainder terms not covered by the finite dimensional reduction. The construction leads to the existence of the periodic solution with the required geometric properties for a large range of parameter values.

Theorem 3 (rigorous computation)**.** *For every $\nu \in [0, 2]$ equation (4) has a periodic solution at energy level $E = 0$ satisfying the geometric properties $\mathcal{H}$.*

The change of variables (3) directly converts Theorems 2 and 3 into Proposition 1.

Numerical simulations suggest that although the parameter range in Theorem 3 (and hence Proposition 1) can be increased somewhat, the solution $\widetilde{u}$ with the described geometric behavior in fact disappears in a saddle node bifurcation at some critical value $\nu_* > 2$ ($\nu_* \approx 2.03$). Hence, one has to find a different mechanism to

force chaos if one wants to prove a similar result for the parameter range $\nu > 2$ (or e.g. $\alpha \in (0, 2]$).

We are going to employ Fourier transformation, a finite dimensional reduction, and a Newton-like operator, which we will prove is a contraction map via rigorous estimation of the tail term. This method has been successfully used in [14] and [17], but here we need to extend it considerably in three crucial aspects. First, the requirement $E = 0$ means that, besides satisfying the differential equation, the solution must obey an additional requirement. This means that the period of the periodic solution cannot be fixed a priori, and instead is another unknown. The extra equation leads, at a more technical level, to the need for better convolution estimates (see Appendix A). Second, rigorous continuation is required in order to not just obtain result for isolated values of ν (cf. [14, 17, 35]), but for the entire parameter interval $\nu \in [0, 2]$. Note that in [12], a result about an entire parameter interval was also obtained, but at a much more computationally expensive price. Third, the geometric condition $\mathcal{H}$ needs to be verified rigorously to be able to combine the computational effort with the topological argument from Theorem 2, so that $\widetilde{u}$ forces chaotic dynamics.

We give a brief outline of the arguments here; full details can be found in Section 3. Let $\frac{2\pi}{L}$ be the a priori unknown period of the solution $\widetilde{u}$, and let the local minima be attained at $y = 0$ and $y = \frac{\pi}{L}$. The symmetry condition H_4 implies that $u'(0) = 0$, hence evaluating the energy constraint (5) at $y = 0$, reduces (5) to

$$u''(0) = \frac{1}{\sqrt{2}}\big(u(0)^2 - 1\big), \tag{6}$$

where we have used that, since we look for solutions satisfying $\mathcal{H}$, we may assume that $u(0) < 1$ is a non-degenerate minimum, hence $u''(0) > 0$. In view of the symmetries, the Ansatz

$$u(y) = a_0 + 2\sum_{l=1}^{\infty} a_l \cos(lLy)$$

is natural and it reduces (4) to (with $a_{-k} \equiv a_k$)

$$g_k \stackrel{\text{def}}{=} \big[1 + \nu L^2 k^2 - L^4 k^4\big] a_k - \sum_{\substack{k_1+k_2+k_3=k \\ k_i \in \mathbb{Z}}} a_{k_1} a_{k_2} a_{k_3} = 0, \qquad \text{for all } k \geq 0,$$

while (6) becomes

$$e \stackrel{\text{def}}{=} -2L^2 \sum_{l=1}^{\infty} l^2 a_l - \frac{1}{\sqrt{2}} \left[a_0 + 2\sum_{l=1}^{\infty} a_l \right]^2 + \frac{1}{\sqrt{2}} = 0.$$

With the notation $x = (L, a_0, a_1, a_2, \dots)$ and $f(x, \nu) = (e, g_0, g_1, g_2, \dots)$, we are thus looking for a solution of $f(x, \nu) = 0$. In this formulation, and using a finite dimensional reduction, we may now use the classical predictor-corrector algorithm for following a continuous branch. However, we need to add a validation step (see [14]) and interval arithmetic to make this into a mathematically rigorous proof. We stress that the interval arithmetic, although necessary and time consuming, is of much less practical importance than the analytic error estimates due to the finite dimensional reduction. Using this finite dimensional reduction, we can, with the help of a computer, find an approximate solution $\bar{x}$ of $f(x, \bar{\nu}) = 0$, as well as an approximate solution $\dot{x}$ of

$\partial_x f(\bar{x}, \bar{\nu})\dot{x} + \partial_\nu f(\bar{x}, \bar{\nu}) = 0$. We also compute an approximate inverse J of $\partial_x f(\bar{x}, \bar{\nu})$. Via rigorous estimates on the remainder terms we show that

$$T(x, \Delta_\nu) = x - Jf(x, \bar{\nu} + \Delta_\nu)$$

is a contraction map on a small ball around $\bar{x} + \Delta_\nu \dot{x}$ in an appropriate Banach space, for all sufficiently small Δ_ν. Repeating this for many small parameter intervals leads us to the existence of a symmetric periodic solution for all $\nu \in [0, 2]$, and, once we have verified the geometric conditions $\mathcal{H}$, to a proof of Theorem 3. It should be clear from the reformulation above that it is quite natural to do parameter continuation. In fact, we expect to find a *continuous* branch of solutions parametrized by ν. Although continuity is easy to verify for each continuation step separately, and indeed this property is used in Section 4 to reduce the amount of computations required, we do not need a globally (i.e., for all $\nu \in [0, 2]$) continuous branch for our proof. We refer to [5] for a general view at obtaining globally continuous branches of solutions using these techniques in the more general context of pseudo arc-length continuation.

Let us comment on further developments. We prove here that the Poincaré return map from Theorem 2, which is in fact the map that follows solutions from one local minimum to the next (see Section 2.1), has topological entropy of at least 0.48. It is possible to obtain better bounds on the entropy, still based on the existence of the periodic solution $\widetilde{u}$, using the $u \to -u$ mirror symmetry, but we will not go into the details here. Furthermore, an analysis along the lines of [4] may lead to statements about the size of the attractor for boundary value problems associated to the PDE (1), all enabled by the rigorous establishment of a single periodic solution with the geometric properties $\mathcal{H}$. This is currently under investigation.

The outline of this paper is as follows. As already noted, it suffices to prove Theorems 2 and 3, which together imply Proposition 1. The forcing Theorem 2 is proved in Section 2. The method that leads to the existence of the special solution described in Theorem 3 is explained in detail in Section 3. Furthermore, Section 4 deals with the verification of the geometric properties $\mathcal{H}$. The analytic estimates in Sections 3 and 4 lead to an algorithm, in which a finite set of inequalities needs to be checked, which is left to a computer program (with interval arithmetic). The estimates together with the output from the computer program prove Theorem 3. The Appendix contains some general and rather sharp convolution estimates needed for the analytic bounds on the remainder terms.

Additional files comes with the paper. The *Matlab* functions *SH_continuation.m*, *SH_rigorous_continuation.m*, *SH_mesh_generator.m*, *SH_geometric_properties.m* and *SH_run_proof.m* rigorously verify Procedures 16 and 21. Furthermore, the movie *SH_geometry_movie.mp4* shows the evolution of the rigorously computed periodic solution, as we move the parameter from $\nu = 0$ to $\nu = 2$. In Section 3.1, details about the computer implementation of the rigorous verification of Procedures 16 and 21 are given, together with a brief description of the *Matlab* functions.

2 Forcing Theorem

In this section we assume, as in Theorem 2, that $\nu \in [0, \sqrt{8})$ and that there exists a periodic solution $\widetilde{u}$ of (4) at $E = 0$ with the geometric properties $\mathcal{H}$. The idea behind the proof is that we code periodic solutions u of (4) at $E = 0$ by their extrema (see Figure 3). This leads to a discretization of the problem. If $u' = 0$, then, by (5), $u'' = \pm\frac{1}{\sqrt{2}}(u^2 - 1)$. Hence, extrema are non-degenerate except at $u = \pm 1$, and we are

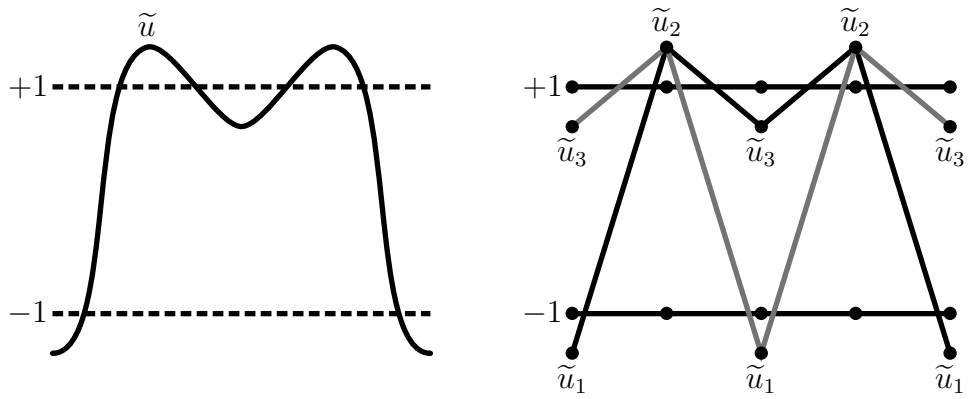

Figure 3: Left: sketch of the solution $\widetilde{u}$. Right: discretized version $\{\widetilde{u}_i\}_{i=1}^4$ and a shift $\{\widetilde{u}_{i+2}\}_{i=1}^4$.

going to avoid those values, so we may for the moment assume all extrema to be non-degenerate. We denote the sequence of extrema of u by $\{u_i\}_{i\in\mathbb{Z}}$, where u_i represents a local minimum for odd i and a local maximum for even i (see also Figure 3).

For $\nu \geq 0$ our system is a so-called Twist systems on $E = 0$, as defined and proved in [3]. The fact that the energy level is singular (contains equilibria) leads to some technical complications, but we shall overcome them relatively easily in our present context. We can therefore use the braid theory for discretized parabolic equations from [18]. The results about Twist systems that are needed in this paper, are summarized in the next lemma; its proof can be found in [3] and [18, Th. 37].

Lemma 4. *Let $\nu > 0$. There exist functions $\mathcal{R}_i \in C^1(\Omega_i;\mathbb{R})$ with domains*

$$\Omega_i = \big\{(u,v,w) \in \mathbb{R}^3 \;\big|\; (-1)^i u < (-1)^i v, (-1)^i w < (-1)^i v, \text{ and } u,v,w \neq \pm 1\big\},$$

with the following properties:

(a) *$\mathcal{R}_{i+2} = \mathcal{R}_i$, so there are really only two different functions in play.*

(b) *$(\mathcal{R}_i)_{i\in\mathbb{Z}}$ is a* parabolic recurrence relation*, i.e., it has the monotonicity property*

$$\partial_{u_{i-1}}\mathcal{R}_i > 0 \qquad \text{and} \qquad \partial_{u_{i+1}}\mathcal{R}_i > 0. \tag{7}$$

(c) *Define*

$$\Omega = \big\{(u_i)_{i\in\mathbb{Z}} \;\big|\; (u_{i-1},u_i,u_{i+1}) \in \Omega_i \text{ for all } i\big\}.$$

A sequence $(u_i)_{i\in\mathbb{Z}} \in \Omega$ solves

$$\mathcal{R}_i(u_{i-1},u_i,u_{i+1}) = 0 \qquad \text{for all } i,$$

if and only if *it corresponds to solution of (4) at $E = 0$ with non-degenerate extrema u_i.*

The shapes of the domains Ω_i reflect the fact that minima are preceded and followed by maxima (and vice versa). The lemma thus implies that instead of looking for (periodic) solutions of (4) at $E = 0$ with non-degenerate extrema, we may try to find (periodic) sequences u_i that solve $\mathcal{R}_i = 0$. We remark that Lemma 4 (and the

method in this paper) extends to a more general class of fourth order ODEs, namely those derived from a second order Lagrangian satisfying the Twist property, see [3]. The Twist property, in essence, means that there are unique monotone solutions of the ODE between extremal values u_i and u_{i+1}.

We want to exploit the fact that the energy level $E = 0$ contains the equilibria $u = \pm 1$. However, these solutions do not correspond to a proper sequence of extrema. The linearization around the equilibria is going to help us resolve this issue. Namely, for $-\sqrt{8} < \nu < \sqrt{8}$ the equilibria ± 1 are saddle-foci, and this leads to the following fact (formulated here for the equilibrium $+1$).

Lemma 5. *Let $-\sqrt{8} < \nu < \sqrt{8}$. For any $\varepsilon > 0$ there exists a sequence $\{u_i^\varepsilon\}_{i=1}^\infty$,*

$$0 < (-1)^i(u_i^\varepsilon - 1) < \varepsilon,$$

which satisfies

$$\mathcal{R}_i(u_{i-1}^\varepsilon, u_i^\varepsilon, u_{i+1}^\varepsilon) = 0 \qquad \text{for } i \geq 2.$$

Notice that we do not claim that $\mathcal{R}_1(u_0^\varepsilon, u_1^\varepsilon, u_2^\varepsilon) = 0$; we did not even define u_0^ε.

Proof. The idea is that the u_i^ε are the extrema of an orbit in the stable manifold of $+1$, which is contained in the energy level $E = 0$. That $u_i^\varepsilon - 1$ alternates sign, follows from the fact that the equilibrium $+1$ is a saddle-focus: it is easy to check that for $-\sqrt{8} < \nu < \sqrt{8}$ the *linearized* equation (i.e., $u = 1+v$ with $v'''' + \nu v'' + 2v + O(v^2) = 0$) has solutions of the form

$$1 + Ce^{-\lambda_r x}\cos(\lambda_i x + \phi),$$

with C and ϕ arbitrary (with $\lambda_r, \lambda_i > 0$ depending on ν). In particular, the stable manifold of the linearized problem intersects the hyperplane $\{u' = 0\}$ in the line

$$\ell = \big\{(1 + v, 0, -\sqrt{2}\, v, 2\sqrt{2}\lambda_r v) \,\big|\, v \in \mathbb{R}\big\}.$$

For the nonlinear equation we need to invoke the stable manifold theorem. Let us denote the stable manifold by $W^s(+1)$ and the local stable manifold by $W^s_{\text{loc}} = W^s(+1) \cap B_{\varepsilon_0}(+1)$ for $\varepsilon_0 > 0$ chosen sufficiently small (so that the following arguments hold). By the stable manifold theorem, the local stable manifold intersects the hyperplane $\{u' = 0\}$ in a curve tangent to ℓ, and thus

$$W^s_{\text{loc}} \cap \{u' = 0\} \subset \big\{(1 + v, 0, -\sqrt{2}\, v + O(v^2), 2\sqrt{2}\lambda_r v + O(v^2)) \,\big|\, v \in \mathbb{R}\big\} \cap B_{\varepsilon_0}(+1).$$

In particular, for ε_0 sufficiently small, for solutions u in the local stable manifold it holds that if $u' = 0$ and $u > 1$ then $u'' < 0$, whereas if $u' = 0$ and $u < 1$ then $u'' > 0$. This shows that all solutions in the local stable manifold have successive extrema on alternating sides of $u = 1$. Now pick one orbit in the local stable manifold and denote its extrema by $\{u_i^{\varepsilon_0}\}_{i=1}^\infty$, with $u_1^{\varepsilon_0}$ a local minimum. Then $0 < (-1)^i(u_i^{\varepsilon_0} - 1) < \varepsilon_0$, and $u_i^{\varepsilon_0} \to 1$ as $i \to \infty$ (exponentially fast in fact). For $\varepsilon < \varepsilon_0$ we may choose $u_i^\varepsilon = u_{i+2n(\varepsilon)}^{\varepsilon_0}$ for some $n(\varepsilon) \in \mathbb{N}$ sufficiently large. □

We can use the symmetry to obtain an analogous result near -1. To be explicit, $\bar{u}_i^\varepsilon = -u_{i+1}^\varepsilon$ satisfies $0 < (-1)^i(\bar{u}_i^\varepsilon + 1) < \varepsilon$. For "technical" reasons to become clear later, we will need to shift this solution, modulo the $2p$-periodicity:

$$\hat{u}_i^\varepsilon = \bar{u}_{i-2 \bmod 2p}^\varepsilon. \tag{8}$$

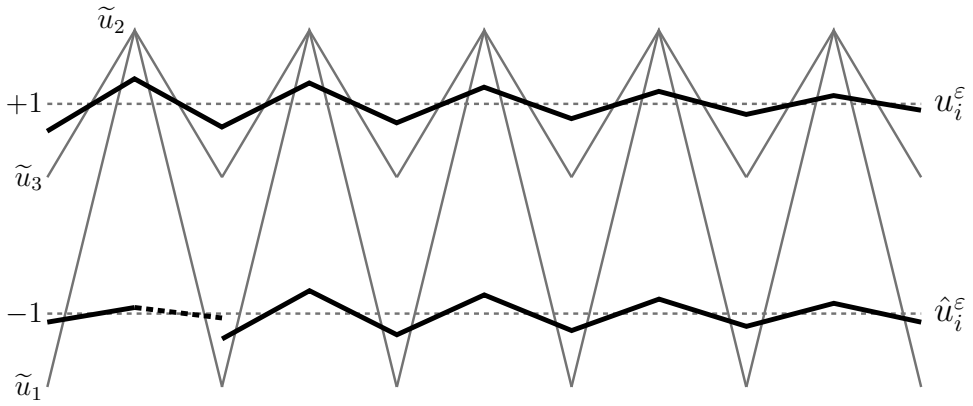

Figure 4: The "up-down" setting including the oscillating tails in the local stable manifolds of ± 1.

In fact, we have not yet chosen the period of the sequences/solutions under scrutiny, but we will do so shortly. See Figure 4 for an illustration of u_i^ε and $\hat{u}_i^\varepsilon$. Notice that $\hat{u}_i^\varepsilon$ does not "close" at $i = 3$. Nevertheless, this will not stop us from putting it to use below.

To study solutions of $\mathcal{R}_i = 0$ we introduce an artificial new time variable s, and consider $u_i(s)$ evolving according to the flow $u_i' = \mathcal{R}_i$. Clearly, we want to find stationary points, and we are going to construct isolating neighborhoods for the flow (any $p \in \mathbb{N}$)

$$\frac{du_i}{ds} = \mathcal{R}_i(u_{i-1}, u_i, u_{i+1}), \qquad i = 1, \dots, 2p, \tag{9}$$

where we identify $u_0 = u_{2p}$ and $u_1 = u_{2p+1}$. The monotonicity property (7) implies that this flow has the decreasing intersection-number property: if two solutions are represented as piecewise linear functions (as in most of the figures), then the number of intersections can only decrease as time s increases.

To build the isolating neighborhoods for (9), consider first the solution $\widetilde{u}$ with geometric properties $\mathcal{H}$. Since it is a periodic solution of (4) at $E = 0$, it follows from Lemma 4c that (recall that $\widetilde{u}_2 = \widetilde{u}_4$)

$$\begin{aligned}
\mathcal{R}_1(\widetilde{u}_2, \widetilde{u}_1, \widetilde{u}_2) &= 0,\\
\mathcal{R}_2(\widetilde{u}_1, \widetilde{u}_2, \widetilde{u}_3) &= 0,\\
\mathcal{R}_1(\widetilde{u}_2, \widetilde{u}_3, \widetilde{u}_2) &= 0,\\
\mathcal{R}_2(\widetilde{u}_3, \widetilde{u}_2, \widetilde{u}_1) &= 0.
\end{aligned}$$

Next, we choose

$$\varepsilon = \frac{1}{2}\max\{-1 - \widetilde{u}_1, \widetilde{u}_2 - 1, 1 - \widetilde{u}_3\}.$$

Although not strictly necessary for understanding the arguments that follow, it is worth mentioning that in the setting of discretized braids described in [18], we are going to use a skeleton consisting of four strands (see Figure 3, right, and Figure 4): $v_i^1 = \widetilde{u}_i$ and $v_i^2 = \widetilde{u}_{i+2}$, and $v_i^3 = u_i^\varepsilon$ and $v_i^4 = \hat{u}_i^\varepsilon$. To be precise, both v^1 and v^2 are defined for all $i \in \mathbb{Z}$ and are 4-periodic. Furthermore, v^3 is defined for all $i \geq 1$

(though not periodic), while v^4 is defined for $i = 0, \dots 2p+1$, with $v_0^4 = v_{2p}^4$ and $v_{2p+1}^4 = v_1^4$. All four strands satisfy

$$\mathcal{R}_i(v_{i-1}, v_i, v_{i+1}) = 0 \qquad \text{for } i = 1, \dots, 2p,$$

with the *exception* of v^3 at $i = 1$, and v^4 at $i = 2, 3$. Below we will make sure that these points do not come into play in the construction of isolating neighborhoods.

Consider a finite, but arbitrarily long sequence

$$\mathbf{a} = \{\mathbf{a}_j\}_{j=1}^N, \qquad \mathbf{a}_j \geq 2. \tag{10}$$

Let the period of the sequences (u_i) be $p = \sum_{j=1}^N \mathbf{a}_j$. Now that p is fixed, the meaning of $\hat{u}_i^\varepsilon$ in (8) is settled. We define the set of partial sums

$$\mathcal{A} = \Big\{ \sum_{j=1}^{n-1} \mathbf{a}_j \;\Big|\; n = 1, \dots, N \Big\}.$$

Note that $0 \in \mathcal{A}$. Now define the set (neighborhood) $U_\mathbf{a} \subset \mathbb{R}^{2p}$ as a product of intervals

$$U_\mathbf{a} = \{u_i \in I_i, i = 1, \dots, 2p\},$$

where the intervals are given by

$$\begin{aligned}
I_i &= [u_i^\varepsilon, \widetilde{u}_2], \qquad \text{if } i \text{ is even;} \\
I_i &= [\widetilde{u}_3, u_i^\varepsilon], \qquad \text{if } i \text{ is odd and } \frac{i-1}{2} \notin \mathcal{A}; \\
I_i &= [\widetilde{u}_1, \hat{u}_i^\varepsilon], \qquad \text{if } i \text{ is odd and } \frac{i-1}{2} \in \mathcal{A}.
\end{aligned}$$

Notice that $U_\mathbf{a}$ is contained in the domain of definition Ω of $\mathcal{R}$, since ± 1 are not in any of the intervals I_i, and the "up-down" criterion is also satisfied (the intervals I_i for odd i lie strictly below the ones for even i). It is useful to review the intervals in the context of Figure 4, and to look at Figure 6 for an example with $\mathbf{a} = 243$.

We now prove that every $U_\mathbf{a}$ contains an equilibrium of (9), still under the assumption that $\widetilde{u}$ is a periodic solution of (4) at $E = 0$ with geometric properties $\mathcal{H}$.

Lemma 6. *For any* $\mathbf{a}$ *defined in (10) the set* $U_\mathbf{a}$ *contains an equilibrium, corresponding to a periodic solution of (4) on* $E = 0$.

Proof. The case $\mathbf{a} = 222 \dots 2 = 2^q$ is exceptional, since the point $(\widetilde{u}_1, \widetilde{u}_2, \widetilde{u}_3, \widetilde{u}_2)^q$, corresponding to the periodic solution $\widetilde{u}$, lies on the boundary of (the closed set) $U_{222\dots2}$.

For all other $\mathbf{a}$, the corresponding solution lies in the interior of $U_\mathbf{a}$. The proof follows from the general theory in [18]. Namely, suppose from now on that $\mathbf{a} \neq 222 \dots 2$. Then $U_\mathbf{a}$ is an isolating block for the flow in the sense of the Conley index, and the flow points outwards everywhere on the boundary. This is relatively easy to check on the co-dimension 1 boundaries of $U_\mathbf{a}$, i.e., exactly one of the u_i lies on the boundary of I_i, while all the others are in the interior; for the higher co-dimension boundaries, see [18]. For the following arguments it may be helpful for the reader to consult Figure 5.

Let us consider one of the sides of the $2p$-cube $U_\mathbf{a}$, for example $u_i = u_i^\varepsilon$ for some even i, i.e., u_i is on the lower boundary of I_i. Since $u_{i-1} < u_{i-1}^\varepsilon$, and $u_{i+1} < u_{i+1}^\varepsilon$ on the co-dimension 1 piece of this side, we infer from the monotonicity (7) that

$$\frac{du_i}{ds} = \mathcal{R}_i(u_{i-1}, u_i, u_{i+1}) < \mathcal{R}_i(u_{i-1}^\varepsilon, u_i^\varepsilon, u_{i+1}^\varepsilon) = 0.$$

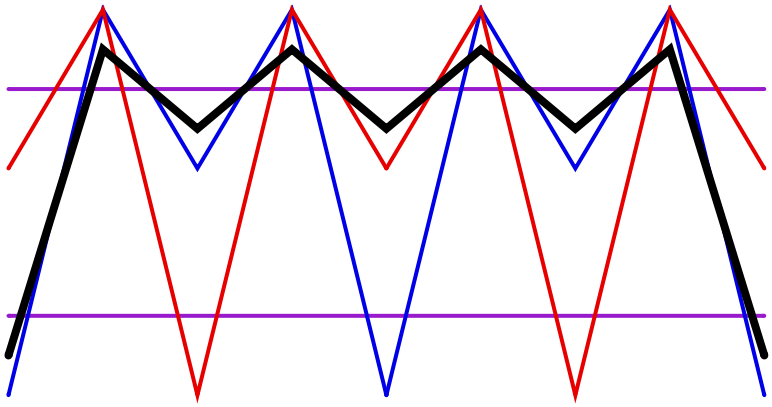

Figure 5: The thin colored lines denote the skeleton, where we represent u^ε and $\hat{u}^\varepsilon$ by constants for convenience. The thick black lines represent the free strand, which is in $U_{\mathbf{a}}$ for $\mathbf{a} = (4)$, $p = 4$. One can check that on the boundary of $U_{\mathbf{a}}$ the number of crossings with at least one of the skeletal strands decreases, hence the flow points outwards on the boundary $\partial U_{\mathbf{a}}$.

Hence the flow points outwards. And when $u_i = \widetilde{u}_2$ for some even i (the upper boundary point of I_i), then, since $\mathbf{a}_j \geq 2$, either $\frac{i-1}{2} \notin \mathcal{A}$ or $\frac{i+1}{2} \notin \mathcal{A}$, or both. Let us consider the case $\frac{i-1}{2} \notin \mathcal{A}$ (the other case is analogous), then $u_{i-1} > \widetilde{u}_3$ and $u_{i+1} > \widetilde{u}_1$ (assuming again that $(u_i)_{i=1}^{2p}$ is in a co-dimension 1 boundary), hence

$$\frac{du_i}{ds} = \mathcal{R}_i(u_{i-1}, u_i, u_{i+1}) > \mathcal{R}_2(\widetilde{u}_3, \widetilde{u}_2, \widetilde{u}_1) = 0,$$

and thus the flow points outwards again. All other (co-dimension 1) boundaries can be dealt with analogously.

We should note that, by construction of the neighborhoods in combination with the definition of u^ε and $\hat{u}^\varepsilon$, we avoid the three points where the skeleton does not satisfy the recurrence relation. In particular, no part of the boundary $\partial U_{\mathbf{a}}$ lies in the hyperplanes $u_1 = u_1^\varepsilon$ (since $u_1 < -1$) or $u_2 = \hat{u}_2^\varepsilon$ or $u_3 = \hat{u}_3^\varepsilon$ (since $\mathbf{a}_1 \geq 2$, hence $u_2, u_3 > \widetilde{u}_3$). We leave the remaining details to the reader.

As said before, for the higher co-dimension boundaries we refer to [18, Prop. 11, Th. 15]. We can now conclude that since $U_{\mathbf{a}}$ is a $2p$-cube and the flow points outwards on $\partial U_{\mathbf{a}}$, its Conley index is homotopic to a $2p$-sphere, and the non-vanishing of its Euler characteristic implies that there has to be a stationary point in the interior of $U_{\mathbf{a}}$ [18, Lem. 36], corresponding to a solution of (4) by Lemma 4c. □

Remark 7. A similar result holds for energy levels close to $E = 0$. The main difference is that the infinite sequences u_i^ε, consisting of the extrema of a solution in the stable manifold of 1, is not available in energy levels $E \neq 0$. Nevertheless, an analogous construction can be set up for E sufficiently close to 0, *provided* the sequences $\mathbf{a} = \{\mathbf{a}_j\}_{j=1}^N$ are now chosen with $2 \leq \mathbf{a}_j \leq N_E < \infty$, where N_E tends to infinity as E approaches 0. For $E > 0$ (and small) an additional difficulty arises, because the Twist property (and hence Lemma 4) does not immediately follow from the results in [3]. However, perturbation methods can be used to show that the Twist

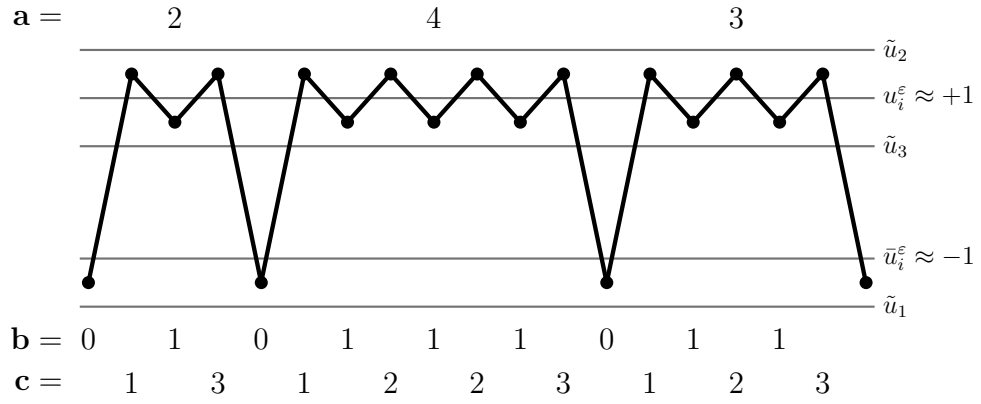

Figure 6: A schematic example of a pattern in $U_{\mathbf{a}}$, with at the top the coding $\mathbf{a}$, and below the corresponding codings $\mathbf{b}$ and $\mathbf{c}$, which are used in the discussion of the entropy.

property persists for small $E > 0$, at least away from the equilibria $u = \pm 1$. The details are beyond the scope of the current paper.

Remark 8. When the symmetry condition H_4 is dropped, then the definition of $U_{\mathbf{a}}$ needs to be modified to accommodate for the fact that $\widetilde{u}_2 \neq \widetilde{u}_4$. The shape of the set $U_{\mathbf{a}}$ will be more complicated than just a single $2p$-cube. Namely, one needs to consider the appropriate discretized braid class, see [18]. Nevertheless, the results in [18] show that the Conley index of this braid class is again homotopic to a sphere, and Lemma 6 and the results in the next section remain valid in the non-symmetric setting.

2.1 Topological entropy

In this section we construct a semi-conjugacy from a Poincaré section of the flow to a subshift of finite type with positive entropy, and thereby finish the proof of Theorem 2. This process involves a couple of somewhat technical steps.

First, we look at an alternative coding, which is more convenient when examining the entropy. We extend any sequence $\mathbf{a} = \{\mathbf{a}_j\}_{j=1}^N$, $\mathbf{a}_j \geq 2$ periodically to a bi-infinite sequence: $\mathbf{a}_{j+N} = \mathbf{a}_j$. To such a periodic sequence we associate a bi-infinite sequence of 0's and 1's:

$$\mathbf{b} = \cdots 01^{\mathbf{a}_{-2}-1}01^{\mathbf{a}_{-1}-1}01^{\mathbf{a}_0-1}.01^{\mathbf{a}_1-1}01^{\mathbf{a}_2-1}0\cdots .$$

Notice, in particular, that $\mathbf{b}_0 = 0$. This coding is also indicated in Figure 6. It is not hard to see that the sequences $\mathbf{b}$ are in the symbol space Σ_B generated by the adjacency matrix

$$B = \begin{pmatrix} 0 & 1 \\ 1 & 1 \end{pmatrix}.$$

We now interpret $U_{\mathbf{a}}$ as an *infinite* product of intervals, and in terms of $\mathbf{b}$ the intervals

making up the neighborhood $U_{\mathbf{a}} = U_{\mathbf{b}}$ are given by ($i \in \mathbb{Z}$)

$$\begin{aligned} I_i &= [u_i^\varepsilon, \widetilde{u}_2] && \text{if } i \text{ is even,} \\ I_i &= [\widetilde{u}_3, u_i^\varepsilon] && \text{if } i \text{ is odd and } b_{\frac{i+1}{2}} = 0, \\ I_i &= [\widetilde{u}_1, \hat{u}_i^\varepsilon] && \text{if } i \text{ is odd and } b_{\frac{i+1}{2}} = 1. \end{aligned}$$

Let $u_{\mathbf{a}} = u_{\mathbf{b}}$ be the periodic solutions of (4) at $E = 0$ corresponding to the stationary points in $U_{\mathbf{a}} = U_{\mathbf{b}}$, which was found in Lemma 6.

An arbitrary periodic sequence in Σ_B might not have a $b_0 = 0$, but for any periodic sequence $\mathbf{b} \neq 1^\infty$ in Σ_B we can find a periodic solution of (4) at $E = 0$ in $U_{\mathbf{b}}$ by using an appropriate shift.

It is now time to set up the semi-conjugacy from a Poincaré map of the flow to the shift-map σ on Σ_B. It is not difficult to check that the sets $\mathcal{C} \subset \{E = 0\} \subset \mathbb{R}^4$ of all orbits, varying over all possible periodic **a**'s or **b**'s, is uniformly bounded. Taking the closure of this set, we obtain a compact invariant set $\overline{\mathcal{C}}$ for the ODE. Notice that it may include the equilibrium solution $u \equiv 1$.

Next we choose a Poincaré section. The energy level $E = 0$ is a three dimensional subset of the phase space $\mathbb{R}^4$. A local minimum in $E = 0$ is defined by the values of u and u''', since $u'' = \frac{1}{\sqrt{2}}|u^2 - 1|$. The Poincaré section is therefore defined as the two-dimensional subset

$$\mathcal{P} = \Big\{(u, 0, \tfrac{1}{\sqrt{2}}|u^2 - 1|, u''') \,|\, u, u''' \in \mathbb{R}\Big\},$$

and the return map $\mathcal{T} : \mathcal{P} \to \mathcal{P}$ follows solutions from one minimum to the next. For the special point $\pm\mathbf{1} = (\pm 1, 0, 0, 0) \in \mathcal{P}$ we define $\mathcal{T}(\pm\mathbf{1}) = \pm\mathbf{1}$.

Lemma 9. *For any $\nu > -\sqrt{8}$ the Poincaré return map $\mathcal{T}$ is well-defined on $\mathcal{P}$, and $\mathcal{T}$ is continuous.*

Proof. That $\mathcal{T}$ is well-defined, follows from the fact that any solution $u \not\equiv 1$ in $E = 0$ has infinitely many extrema, which was proved in e.g. [26, Lem. 3.1.2]. That $\mathcal{T}$ is continuous away from $\pm\mathbf{1}$ follows from the methods in the proof of Lemmas 3.1.3 and 3.1.4 in [26]. There, only symmetric settings were considered, but the method prevails in the non-symmetric setting. Continuity of $\mathcal{T}$ at $\pm\mathbf{1}$ follows from the fact that the equilibria are either saddle-foci ($|\nu| < \sqrt{8}$) or centers ($\nu \geq \sqrt{8}$). Roughly speaking, the closer an orbit start to ± 1, the more extrema near ± 1 it has. It is not hard to deduce continuity from at $\pm\mathbf{1}$ from this. □

By construction and Lemma 9, the return map $\mathcal{T}$, defined on $\mathcal{P}$, has a compact invariant set $\Lambda = \mathcal{P} \cap \overline{\mathcal{C}}$. For $\lambda \in \Lambda$, we denote by $u^\lambda(y)$ the solution with *initial data* λ.

Lemma 10. *Let $\lambda \in \Lambda$ and let u^λ be the associated solution of (4). Suppose $u^\lambda \not\equiv 1$. Then u^λ has only non-degenerate extrema, with the maxima in $(1, \widetilde{u}_2]$, and the minima either in $[\widetilde{u}_3, 1)$ or in $[\widetilde{u}_1, -1)$.*

Proof. We write $u = u^\lambda$. All solutions in $\overline{\mathcal{C}}$ can be approximated arbitrarily closely (on compact intervals) by the periodic solutions found in Lemma 6. Non-degenerate extrema persist, whereas degenerate extrema ($u' = u'' = 0$) in $E = 0$ must lie on the lines $u = \pm 1$. Hence, the bounds on the extrema follow immediately from the definitions of $U_{\mathbf{a}}$ and I_i, once we have excluded degenerate extrema, i.e., inflection points on $u = \pm 1$.

To rule out inflection points we argue by contradiction (see also [26, Lem. 3.1.5]). Suppose $u \in \overline{\mathcal{C}}$ has an inflection point, say $u'(0) = u''(0) = 0$. Hence $u(0) = \pm 1$ and $u'''(0) \neq 0$ (if $u'''(0) = 0$ then $u \equiv 1$ by uniqueness of the initial value problem). We consider the case $u(0) = 1$ and $u'''(0) > 0$; the other three cases are ruled out in an analogous manner. Let $\{u_n\}_{n=1}^{\infty}$ be a sequence of periodic solutions found in Lemma 6, such that $u_n \to u$ in C^3 on any bounded interval. Then by the implicit function theorem, for large enough n, there exist points y_n such that $\lim_{n\to\infty} y_n = 0$ and $u_n''(y_n) = 0$. We know that $u_n'(y_n) \neq 0$, since the u_n have only non-degenerate extrema.

We now consider two cases: either $u_n'(y_n) > 0$ or $u_n'(y_n) < 0$ for infinitely many of $n \in \mathbb{N}$. In the former case we argue as follows. Taking a subsequence we may assume that $u_n'(y_n) > 0$ for all n. We conclude from $E = 0$ and $u_n''(y_n) = 0$ that

$$u_n'''(y_n) + \frac{\nu}{2} u_n'(y_n) = -\frac{(u_n(y_n)^2 - 1)^2}{4u_n'(y_n)} \leq 0.$$

Taking the limit $n \to \infty$ in the above inequality leads to $u'''(0) + \frac{\nu}{2}u'(0) \leq 0$, which contradicts the assumption that u has an inflection point at $y = 0$ with $u'''(0) > 0$.

In the latter case, we may assume that $u_n'(y_n) < 0$ for all n. Since in the inflection point $u'''(0) > 0$, it follows that $u'(y) > 0$ for $y \neq 0$ sufficiently small. This means that for n large enough there are sequences $y_n^1 < y_n < y_n^2$ of local maxima and minima of u_n, respectively, such that $y_n^{1,2} \to 0$ as $n \to \infty$. Since the periodic solutions u_n have their extrema on alternating sides of $+1$ by construction, there is a sequence $y_n^3 \in (y_n^1, y_n^2)$ such that $u_n(y_n^3) = 1$ and $u_n'(y_n^3) < 0$. We conclude from $E = 0$ and $u_n(y_n^3) = 1$ that

$$u_n'''(y_n^3) + \frac{\nu}{2} u_n'(y_n^3) = \frac{u_n''(y_n^3)^2}{u_n'(y_n^3)} \leq 0,$$

and we reach a contradiction as before by taking the limit $n \to \infty$ in this inequality, thereby concluding the proof. □

To define the semi-conjugacy $\rho : \Lambda \to \Sigma_B$ we consider the solution $u^\lambda(y)$ of (4) with initial data $\lambda \in \Lambda$. If $u^\lambda \equiv 1$, we define $\rho(\lambda) = 1^\infty$. Otherwise, let u_i^λ be the sequence of extrema of u^λ, indexed such that u_1^λ is the minimum corresponding to $\lambda \in \mathcal{P}$. By Lemma 10, this sequence lies in $U_{\mathbf{b}_\lambda}$ for some $\mathbf{b}_\lambda \in \Sigma_B$, and we define $\rho(\lambda) = \mathbf{b}_\lambda$.

It follows from Lemmas 9 and 10 that the map ρ is continuous (also in the point $+\mathbf{1}$, if $+\mathbf{1}$ happens to lie in Λ). Moreover, $\rho \circ \mathcal{T} = \sigma \circ \rho$ by construction and the properties of the return map (where σ is the shift map). Finally, ρ is surjective. Namely, all *periodic* sequences in Σ_B have corresponding solutions in $\overline{\mathcal{C}}$ (and thus in Λ), and since the set of periodic sequences is dense in Σ_B and Λ is compact, surjectivity follows. Hence, ρ defines a semi-conjugacy, and it follows (e.g. [28]) that the topological entropy of the map $\mathcal{T}$ on Λ is positive:

$$h_{\mathrm{top}}\big(\mathcal{T}|_\Lambda\big) \geq h_{\mathrm{top}}\big(\sigma|_{\Sigma_B}\big) = \log\left(\frac{1+\sqrt{5}}{2}\right).$$

This finishes the proof of Theorem 2.

Remark 11. There is another way to make a coding, that was already alluded to in the introduction. The profile between two successive minima can, qualitatively, have

three shapes (see Figure 2):

$$\begin{aligned} u_i < -1 \ \text{ and } \ u_{i+2} > -1, &\qquad \text{coded by } \mathbf{c}_i = 1;\\ u_i > -1 \ \text{ and } \ u_{i+2} > -1, &\qquad \text{coded by } \mathbf{c}_i = 2;\\ u_i > -1 \ \text{ and } \ u_{i+2} < -1, &\qquad \text{coded by } \mathbf{c}_i = 3. \end{aligned}$$

This new coding $\mathbf{c}$ is also indicated in Figure 6. The corresponding adjacency matrix is

$$\begin{pmatrix} 0 & 1 & 1 \\ 0 & 1 & 1 \\ 1 & 0 & 0 \end{pmatrix}.$$

This of course does not improve the bound on the entropy of $\mathcal{T}$, but the slightly more complicated coding $\mathbf{c}$, using "up-down" building blocks, is more intuitively related to the shape of solutions, as expressed in Figure 2.

3 Rigorous Continuation

We are going to restrict our attention to symmetric periodic solutions u satisfying $\mathcal{H}$. Hence, let

$$u(y) = a_0 + 2\sum_{l=1}^{\infty} a_l \cos(lLy), \tag{11}$$

with L an a priori unknown variable. Since $u'(0) = 0$, and the energy (5) is a conserved quantity along the orbits of (4), we get that

$$\begin{aligned} E &= u'''(0)u'(0) - \frac{1}{2}u''(0)^2 + \frac{\nu}{2}u'(0)^2 + \frac{1}{4}(u^2-1)^2 \\ &= -\frac{1}{2}\left[u''(0) - \frac{1}{\sqrt{2}}\big(u(0)^2-1\big)\right]\left[u''(0) + \frac{1}{\sqrt{2}}\big(u(0)^2-1\big)\right]. \end{aligned}$$

Since we look for u such that $E = 0$, $u(0) < -1$ and $u''(0) > 0$, the energy condition boils down to

$$u''(0) - \frac{1}{\sqrt{2}}[u(0)^2 - 1] = 0. \tag{12}$$

Substituting the expansion (11) of $u(y)$ in (12), we obtain

$$e(L,a) \stackrel{\text{def}}{=} -2L^2\sum_{l=1}^{\infty} l^2 a_l - \frac{1}{\sqrt{2}}\left[a_0 + 2\sum_{l=1}^{\infty} a_l\right]^2 + \frac{1}{\sqrt{2}} = 0. \tag{13}$$

Plugging the expansion (11) in (4) and computing the inner product of the resulting equations with each $\cos(kLx)$, $k \geq 0$, we get

$$g_k(L,a,\nu) \stackrel{\text{def}}{=} [1 + \nu L^2k^2 - L^4k^4]a_k - \sum_{\substack{k_1+k_2+k_3=k \\ k_i \in \mathbb{Z}}} a_{k_1}a_{k_2}a_{k_3} = 0, \tag{14}$$

where $a = (a_0, a_1, \dots)$. Define $x = (x_{-1}, x_0, x_1, \dots) = (L, a_0, a_1, a_2, \dots)$, and $g = (g_0, g_1, g_2, \dots)^T$, as well as

$$f(x,\nu) = \begin{bmatrix} e(x) \\ g(x,\nu) \end{bmatrix}. \tag{15}$$

To simplify the presentation, we use the notation $f_{-1} = e$ and $f_k = g_k$ for $k \geq 0$. Now, since we want to use rigorous numerical methods to find pairs (x, ν) such that $f(x, \nu) = 0$, we need to consider a finite dimensional projection of (15). Define $x_F = (x_{-1}, x_0, \cdots, x_{m-1}) = (L, a_0, \cdots, a_{m-1}) \in \mathbb{R}^{m+1}$, and

$$e^{(m)}(x_F) \stackrel{\text{def}}{=} -2L^2 \sum_{l=1}^{m-1} l^2 a_l - \frac{1}{\sqrt{2}} \left[a_0 + 2 \sum_{l=1}^{m-1} a_l \right]^2 + \frac{1}{\sqrt{2}},$$

and

$$g^{(m)}(x_F, \nu) \stackrel{\text{def}}{=} [g_0(x_F, \nu), \cdots, g_{m-1}(x_F, \nu)]^T.$$

The *Galerkin projection* of (15) is defined by

$$f^{(m)}(x_F, \nu) \stackrel{\text{def}}{=} \begin{bmatrix} e^{(m)}(x_F) \\ g^{(m)}(x_F, \nu) \end{bmatrix}.$$

It is important to note that $f^{(m)}$ has both a finitely truncated domain and a finitely truncated co-domain.

We now describe how we can modify the classical, numerical, predictor-corrector algorithm for following a continuous branch of solutions to fit our setting. Suppose that, at parameter value $\nu = \nu_0$, we have used a Newton-like iteration method to numerically find $\bar{x}_F$ such that

$$f^{(m)}(\bar{x}_F, \nu_0) \approx 0. \tag{16}$$

Throughout this paper, Df represents the derivative of f with respect to the x_F- or x-variable. If $(\bar{x}_F, \nu_0)$ is a solution of $f^{(m)}(x_F, \nu) \approx 0$ such that the Jacobian matrix $Df^{(m)}(\bar{x}_F, \bar{\nu})$ is invertible, then, by the implicit function theorem, there exists a unique one-dimensional local continuum of solutions (x_F, ν) such that the solution x_F is locally a function of the parameter ν (near ν_0). Moreover, we may numerically find a *tangent* vector $\dot{x}_F$ to the solution curve at $(\bar{x}_F, \nu_0)$, i.e.,

$$Df^{(m)}(\bar{x}_F, \nu_0)\dot{x}_F + \frac{\partial f}{\partial \nu}^{(m)}(\bar{x}_F, \nu_0) \approx 0. \tag{17}$$

We can then use this tangent vector to obtain a *predictor* $\widehat{x}_F = \bar{x}_F + (\nu_1 - \nu_0)\dot{x}_F$ for the solution at a parameter value ν_1 close to ν_0. The *corrector* then consists of iterating a Newton-like map, with initial point $\widehat{x}_F$, to converge to the zero $\widetilde{x}_F$ of $f^{(m)}(x_F, \nu_1)$, see also Figure 7a. There are two essential problems to overcome in this scheme. First, the result for the finite dimensional truncation needs to be "lifted" to the infinite dimensional setting. This lifting is carried out via "validated continuation" [14], with a final interval arithmetic step. Second, the described method leads to a discrete set of solutions (x, ν), whereas we aim for solutions for a *continuous* range of parameter values, and we describe our approach below.

Denote by $\bar{x}_F = (\bar{L}, \bar{a}_0, \bar{a}_1, \cdots, \bar{a}_{m-1})$ and $\dot{x}_F = (\dot{L}, \dot{a}_0, \dot{a}_1, \cdots, \dot{a}_{m-1})$ the approximate solutions of (16) and (17), respectively, and define their infinite extensions $\bar{x} = (\bar{x}_F, 0, 0, 0, \dots)$ and $\dot{x} = (\dot{x}_F, 0, 0, 0, \dots)$. We define the "linear part" of g_k as

$$\mu_k(L, \nu) \stackrel{\text{def}}{=} 1 + \nu L^2 k^2 - L^4 k^4.$$

Furthermore, let the $(m+1) \times (m+1)$ matrix J_F be the numerically computed inverse of $Df^{(m)}(\bar{x}_F, \nu_0)$, and let 0_F be the $1 \times (m+1)$ row vector $(0, 0, \dots, 0)$. We define

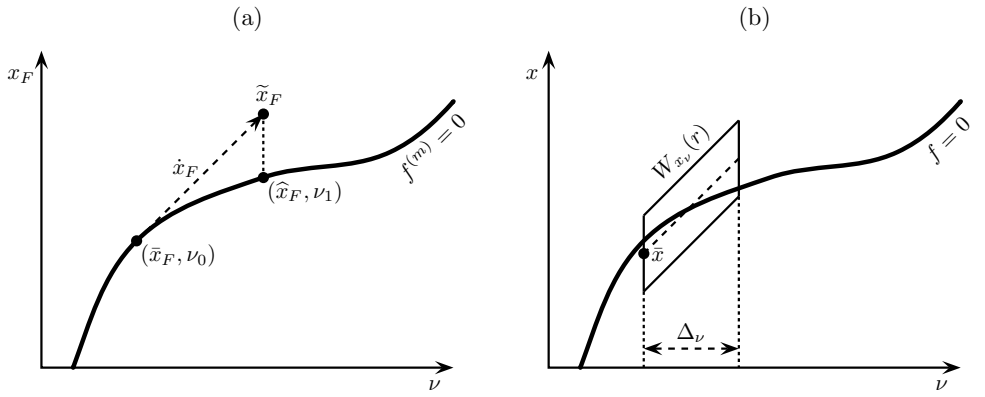

Figure 7: (a) Sketch of the predictor-corrector algorithm for the truncated problem $f^{(m)}(x_F, \nu) = 0$. (b) The neighborhood $W_{x_\nu}(r)$ in which we find solutions of the full problem $f(x, \nu) = 0$.

the linear operator on sequence spaces

$$A \stackrel{\text{def}}{=} \begin{bmatrix} J_F & 0_F^T & 0_F^T & 0_F^T & \cdots \\ 0_F & \mu_m(\bar{L}, \nu_0)^{-1} & 0 & 0 & \cdots \\ 0_F & 0 & \mu_{m+1}(\bar{L}, \nu_0)^{-1} & 0 & \cdots \\ 0_F & 0 & 0 & \mu_{m+2}(\bar{L}, \nu_0)^{-1} & \\ \vdots & \vdots & \vdots & & \ddots \end{bmatrix}, \tag{18}$$

which acts as an *approximate inverse* of the linear operator $Df(\bar{x}, \nu_0)$. We shall always make sure that m is sufficiently large, so that $\mu_m(\bar{L}, \nu_0) < 0$. For ν close to ν_0, we consider the Newton-like operator

$$T_\nu(x) \stackrel{\text{def}}{=} x - A \cdot f(x, \nu). \tag{19}$$

To formalize this approach, it is convenient to use a functional analytic setting. As weight functions we define, for $s > 0$,

$$\omega_k^s = \begin{cases} 1, & k = -1, 0; \\ k^s, & k \geq 1. \end{cases} \tag{20}$$

In general, one can play around with these weight functions (and the norm below); for the problem in this paper, we have found the choice (20) to be appropriate, because it leads to a proof. These weight functions are used in the norms

$$\|x\|_s = \sup_{k=-1,0,1,\ldots} |x_k \omega_k^s|, \tag{21}$$

and the sequence spaces

$$\Omega^s = \{x\,,\, \|x\|_s < \infty\},$$

consisting of sequences with algebraically decaying tails. For the first sum in (13) to make sense, we shall require that $s > 3$.

Lemma 12. *We have the following:*

(a) *The sequence space* Ω^s *with norm* $\|\cdot\|_s$ *is a Banach space for all* s*. The injections* $\Omega^{s_1} \hookrightarrow \Omega^{s_2}$ *are compact for all* $s_1 > s_2$*.*

(b) *Let* $s > 3$*. The map* $T(x, \nu)$ *is continuous from* $\Omega^s \times \mathbb{R}$ *to* Ω^{s+2}*, and* $T(x, \nu)$ *is compact from* $\Omega^s \times \mathbb{R}$ *to* Ω^s*.*

(c) *Let* $s_0 > 3$ *and fix* ν*. Zeros of* $f(x, \nu)$*, or, equivalently, fixed points of* $T(x, \nu)$*, that are in* Ω^{s_0}*, are in* Ω^s *for all* $s \geq s_0$*.*

(d) *Let* $s > 3$*. A sequence* $x = (L, a_0, a_1, \dots) \in \Omega^s$ *is a zero of* f*, or a fixed point of* T*,* if and only if *u given by (11) is a periodic solution of (4) at energy level* $E = 0$*, with period* $\frac{2\pi}{L}$*, and symmetric in* $y = 0$ *and* $y = \frac{\pi}{L}$*.*

Proof. These are straightforward exercises in functional analysis. □

Lemma 12d shows that the problem of finding (symmetric) periodic solutions of (4) at $E = 0$ is equivalent to studying fixed points of T. We will find balls in Ω^s on which T, for fixed ν, is a contraction mapping, thus leading to solutions of (4). Let us define the ball of radius r, centered at the origin,

$$W(r) \stackrel{\text{def}}{=} [-r, r]^2 \times \prod_{k=1}^{\infty} \left[-\frac{r}{k^s}, \frac{r}{k^s}\right]. \tag{22}$$

For $\Delta_\nu = \nu - \nu_0$ small, we define the *predictors based at* ν_0 by

$$x_\nu = \bar{x} + \Delta_\nu \dot{x}.$$

For ν close to ν_0 we define the ball centered at x_ν

$$W_{x_\nu}(r) = x_\nu + W(r).$$

We look for fixed points of T inside these balls/neighborhoods, see also Figure 7b. To show that T is a contraction mapping, we need bounds Y_k and Z_k for all $k = -1, 0, 1, 2, \dots$, such that, with $\Delta_\nu = \nu - \nu_0$,

$$\left|[T_\nu(x_\nu) - x_\nu]_k\right| \leq Y_k(\Delta_\nu), \tag{23}$$

and

$$\sup_{w, w' \in W(r)} \left|[DT_\nu(x_\nu + w')w]_k\right| \leq Z_k(r, \Delta_\nu). \tag{24}$$

We will find such bounds in Sections 3.2 and 3.3, respectively. Notice that $Y_k \geq 0$ and $Z_k \geq 0$. Although not a restriction, we will, in this paper, only consider $\Delta_\nu \geq 0$, since we will initiate the continuation at the parameter value $\nu = 0$ and finish at $\nu = 2$, hence we do continuation in one direction only.

Variants of the following lemma were also used in [12, 14, 17, 34].

Lemma 13. *Fix* $s > 3$ *and* $\nu = \nu_0 + \Delta_\nu$*. If there exists an* $r > 0$ *such that* $\|Y + Z\|_s < r$*, with* $Y = (Y_{-1}, Y_0, Y_1, \dots)$ *and* $Z = (Z_{-1}, Z_0, Z_1, \dots)$ *the bounds as defined in (23) and (24), then there is a unique* $\widetilde{x}_\nu \in W_{x_\nu}(r)$ *such that* $f(\widetilde{x}_\nu, \nu) = 0$*.*

Proof. We outline the proof, which can be found in more detail in [14] and [34]. The mean value theorem (applied component-wise), combined with the assumption $\|Y + Z\|_s < r$, implies that $T(\cdot, \nu)$ maps $W_{x_\nu}(r)$ into itself. Since $Y_k \geq 0$ and $Z_k \geq 0$, it follows that $\|Z\|_s \leq \|Y + Z\|_s < r$. We infer from the mean value theorem that the Lipschitz constant of $T(\cdot, \nu)$ on $W_{x_\nu}(r)$ can be estimated above by $\|Z\|_s / r < 1$, so that T is a contraction mapping. Finally, zeros of f correspond to fixed point of T, hence an application of the Banach fixed point theorem concludes the proof. □

In order to verify the hypotheses of Lemma 13 in a computationally efficient way, we introduce the notion of *radii polynomials*. Namely, as will become clear in Sections 3.2 and 3.3, the functions $Y_k(\Delta_\nu)$ and $Z_k(r, \Delta_\nu)$ are polynomials in their independent variables. Also, for sufficiently large k, say $k \geq M$, one may choose

$$Y_k = 0, \qquad \text{and} \qquad Z_k = \widehat{Z}_M \left(\frac{M}{k}\right)^s,$$

for some $\widehat{Z}_M(r, \Delta_\nu) > 0$. This leads us to the following definition.

Definition 14. *Let $Y_k(\Delta_\nu) = 0$ and $Z_k(r, \Delta_\nu) = \widehat{Z}_M(r, \Delta_\nu)\left(\frac{M}{k}\right)^s$ for all $k \geq M$. We define the $M+2$* radii polynomials $\{p_{-1}, p_0, \ldots, p_{M-1}, p_M\}$ *by*

$$p_k(r, \Delta_\nu) \stackrel{\text{def}}{=} \begin{cases} Y_k(\Delta_\nu) + Z_k(r, \Delta_\nu) - \frac{r}{\omega_k^s}, & k = -1, 0, \ldots, M-1; \\ \widehat{Z}_M(r, \Delta_\nu) - \frac{r}{\omega_M^s} & k = M. \end{cases}$$

The usefulness of the radii polynomials p_k follows from the observation that the polynomials Y_k and Z_k have a few exceptionally small terms. Namely, it turns out that they are *roughly* of the form (to be made precise in see Sections 3.2 and 3.3)

$$\begin{aligned} Y_k &\sim \delta_1 + \delta_2 \Delta_\nu + O(\Delta_\nu^2), \\ Z_k &\sim \delta_3 r + O(\Delta_\nu r, r^2), \end{aligned}$$

where the δ_1, δ_2 and δ_3 are small, because of the choice of $\bar{x}$, the choice of $\dot{x}$, and the choice of the linear operator A in the map Newton-like map T, respectively. It is easy to see that the zeroth order term of Z_k vanishes. Hence, the radii polynomials are roughly of the form

$$p_k(r, \Delta_\nu) \sim (\delta_1 + \Delta_\nu \delta_2) - \left(\frac{1}{\omega_k^s} - \delta_3\right) r + O(r^2, \Delta_\nu r, \Delta_\nu^2),$$

so that one may anticipate them to be negative for small r (but not too small) for a reasonably large range of Δ_ν.

Lemma 15. *Let $s > 3$ and let $Y_k(\Delta_\nu) = 0$ and $Z_k(r, \Delta_\nu) = \widehat{Z}_M(r, \Delta_\nu)\left(\frac{M}{k}\right)^s$ for all $k \geq M$. Suppose that there exists an $r > 0$ such that $p_k(r, \Delta_\nu) < 0$ for all $k = -1, \ldots, M$, then the hypotheses of Lemma 13 are satisfied for $\nu = \nu_0 + \Delta_\nu$.*

Proof. Let $s > 3$, $r > 0$ and $\nu = \nu_0 + \Delta_\nu$ such that $p_k(r, \Delta_\nu) < 0$ for all $k = -1, 0, \ldots, M$. Since $Y_k + Z_k = \widehat{Z}_M\left(\frac{M}{k}\right)^s$ for $k \geq M$, by definition of the radii polynomials, we get that

$$\begin{aligned} \|Y + Z\|_s &= \sup_{k=-1,0,1,\ldots} |[Y_k(r) + Z_k(r, \Delta_\nu)]\omega_k^s| \\ &= \max_{k=-1,0,\ldots,M} \{p_k(r, \Delta_\nu)\omega_k^s + r\} < r. \end{aligned}$$

□

Combining Lemmas 13 and 15, it should now become clear that proving the existence of zeros of f, and hence periodic solutions of (4) at $E = 0$, is *computable*, since only a finite number of polynomial inequalities need to be verified. There is one final observation to be made. The Y_k and the Z_k are monotonically increasing in the variable $\Delta_\nu \geq 0$, that is $Y_k(\Delta_\nu^0) \leq Y_k(\Delta_\nu^1)$ and $Z_k(r, \Delta_\nu^0) \leq Z_k(r, \Delta_\nu^1)$ for

$0 \leq \Delta_\nu^0 \leq \Delta_\nu^1$. As a consequence, the same property holds for the radii polynomials: if $0 \leq \Delta_\nu^0 \leq \Delta_\nu^1$, then $p_k(r, \Delta_\nu^0) \leq p_k(r, \Delta_\nu^1)$ for all $k = -1, \ldots, M$. Hence, if the hypotheses in Lemma 13 are satisfied for some $\Delta_\nu^0 > 0$, then they are satisfied for all $\Delta_\nu \in [0, \Delta_\nu^0]$, hence there are corresponding periodic solutions of (4) for all $\nu \in [\nu_0, \nu_0 + \Delta_\nu^0]$.

For what follows we recall that the construction of the radii polynomials p_k involves Y_k and Z_k, defined in (26) and (31), respectively, as well as M_0 and $\widehat{Z}_M$, defined in (30) and (32), respectively. Furthermore, because the coefficients of the polynomials Y_k and Z_k are all positive, there is at most one interval in the positive half line on which p_k is negative. With these considerations in mind, the following procedure leads to a proof of the existence part of Theorem 3. The geometric properties $\mathcal{H}$ will be checked in Procedure 21 in Section 4.

Procedure 16. *To check the hypotheses in Lemma 15 on the interval $\nu \in [0, 2]$ we proceed as follows.*

1. *Choose minimum and maximum step-sizes $0 < \Delta_{\min} < \Delta_{\max}$. Initiate $s > 3$, $m \in \mathbb{N}$, $M \geq \max\{3m - 2, 6\}$, $\nu_0 = 0$, $\Delta_\nu \in [\Delta_{\min}, \Delta_{\max}]$, $\Delta_\nu^0 = 0$, and an approximate zero $\widehat{x}_F$ of $f^{(m)}(x_F, 0)$. Calculate the analytic estimates (α_k, $k = 0, \ldots, M$) that are independent of everything.*

2. *With a classical Newton iteration, find near $\widehat{x}_F$ an approximate solution $\bar{x}_F$ of $f^{(m)}(x_F, \nu_0) = 0$. Calculate an approximate solution $\dot{x}_F$ of (17). Use the first component of $\bar{x}_F$ to calculate with interval arithmetic $M_0(\bar{L}, \nu_0)$, and check that $M_0 \leq M$ (this is never a problem in practice).*

3. *Compute, using interval arithmetic, the coefficients of the radii polynomials p_k, $k = -1, \ldots, M$. This is the computationally most expensive step, since it involves the coefficients in Tables 1, 3 and 4, and in particular requires the calculation of convolution terms.*

4. *Calculate numerically $I = [I_-, I_+] \stackrel{\text{def}}{=} \bigcap_{k=-1}^{M} \{r > 0 \,|\, p_k(r, \Delta_\nu) < 0\}$.*
   - *If $I = \varnothing$ then go to Step 6.*
   - *If $I \neq \varnothing$ then let $r = \frac{11}{10} I_-$. Compute with interval arithmetic $p_k(r, \Delta_\nu)$. If $p_k(r, \Delta_\nu) < 0$ for all $k = -1, \ldots, M$ then go to Step 5; else go to Step 6.*

5. *Update $\Delta_\nu^0 \leftarrow \Delta_\nu$ and $r_0 \leftarrow r$. If $\frac{10}{9}\Delta_\nu \leq \Delta_{\max}$ then update $\Delta_\nu \leftarrow \frac{10}{9}\Delta_\nu$ and go to Step 4; else go to Step 7.*

6. *If $\Delta_\nu^0 > 0$ then go to Step 7; else if $\frac{9}{10}\Delta_\nu \geq \Delta_{\min}$ then update $\Delta_\nu \leftarrow \frac{9}{10}\Delta_\nu$ and go to Step 4; else go to Step 8.*

7. *The continuation step has succeeded. Store, for future reference, $\bar{x}_F$, $\dot{x}_F$, r_0, ν_0 and Δ_ν^0. Determine ν_1 approximately equal to, but interval arithmetically less than, $\nu_0 + \Delta_\nu^0$. If $\nu_1 \geq 2$ then terminate the procedure* successfully*; else make the updates $\nu_0 \leftarrow \nu_1$, $\Delta_\nu \leftarrow \Delta_\nu^0$, $\widehat{x}_F \leftarrow \bar{x}_F + \Delta_\nu^0 \dot{x}_F$, and $\Delta_\nu^0 \leftarrow 0$, and go to Step 2 for the next continuation step.*

8. *The continuation step has failed. Either decrease $\Delta_{\min}$ and return to Step 6; or increase s or M and return to Step 3; or increase m and return to Step 2. Alternatively, terminate the procedure* unsuccessfully *at $\nu = \nu_0$ (although with success on $[0, \nu_0]$).*

During the procedure, a sequence of intervals $[\nu_0, \nu_0 + \Delta_\nu^0]$ covering $[0, 2]$ is stored, together with the variables defining the neighborhoods $W_{x_\nu}(r_0)$. In Section 4, the balls $W_{x_{\nu_0}}(r_0)$ will be used in Procedure 21 (and Lemma 22) to check the geometric conditions $\mathcal{H}$. Concerning the usefulness of the procedure in practice, the proof of the pudding is in the eating.

Lemma 17. *Let $s = 4$, $m = 43$, $M = 127$, $\Delta_{\min} = 10^{-10}$ and $\Delta_{\max} = 2$. Then we can choose an approximate zero $\widehat{x}_F = \widehat{x}_F^*$ of $f^{(m)}(x_F, 0)$ such that Procedure 16 terminates* successfully. *Hence there are periodic solutions of (4) at $E = 0$ for all $\nu \in [0, 2]$.*

The choice of $\widehat{x}_F^*$ is made in such a way that the solutions found satisfy the geometric conditions $\mathcal{H}$. This is checked using Procedure 21.

Proof. A *Matlab* computer program successfully performing Procedure 16 accompanies the paper. In particular, we never end up in Step 8 of the procedure. Concerning the implementation, the only difficult evaluations are the convolution terms, which can be computed in a very efficient way using the fast Fourier transform combined with interval arithmetic, see [17]. More details about the implementation are given in Section 3.1. □

3.1 Implementation

In this section, we discuss in detail the implementation of the rigorous verification of Procedure 16 and Procedure 21 (which checks the geometric properties $\mathcal{H}$, see Section 4). First of all, as seen in [14], the errors induced by the floating point computations of the coefficients of the radii polynomials are small. Hence, finding a positive r at which all radii polynomials are negative without interval arithmetic, gives significant confidence about the success of Procedure 16. On top of that, the computational efficiency of floating point arithmetic in *Matlab* allows for fast computations. With this in mind, we wrote a preliminary function called *SH_continuation.m*, which verifies, without interval arithmetic, that Procedure 16 performs successfully. Using the values given in Lemma 17, we obtained 13068 successful non-rigorous steps in a bit more than 7 minutes. In Figure 8, we plot the evolution of Δ_ν as the parameter ν runs from 0 to 2.

This being done, and armed with confidence, we then aimed for the proof. First we wrote *SH_rigorous_continuation.m*, the equivalent of *SH_continuation.m*, in the *Matlab* interval arithmetic package *Intlab* (see [19]). We did not try to optimize for speed in the interval arithmetic setting, since we preferred to keep the changes with respect to the floating point version *SH_continuation.m* limited. The speed of the interval arithmetic is thus rather slow, and we decided to distribute the computations over 20 different computers, each running 3 simultaneous calculations. Hence, we used the 13068 output points from *SH_continuation.m* to generate a non-uniform mesh $\{(\nu_j, x_j) \,|\, j = 1, \ldots, 61\}$ of the branch under study, where $\nu_1 = 0$ and $\nu_{61} = 2$. The function *SH_mesh_generator.m* picks 61 points out of the 13068 defining the discrete branch. Note that we do not need to define x_{61}, since at this point we have already reached $\nu = 2$. This mesh is stored in the file *SH_mesh_points.mat*. Then, for each $j = 1, \ldots, 60$, we called the function *SH_run_proof*(j). This function first starts *Intlab*, loads *SH_mesh_points.dat*, and then rigorously verifies Procedure 16 between the parameter values ν_j and ν_{j+1}, using *SH_rigorous_continuation.m* with the initial point x_j as input. Finally, it verifies, by running the interval arithmetic function *SH_geometric_properties.m*, that the periodic orbits rigorously generated by

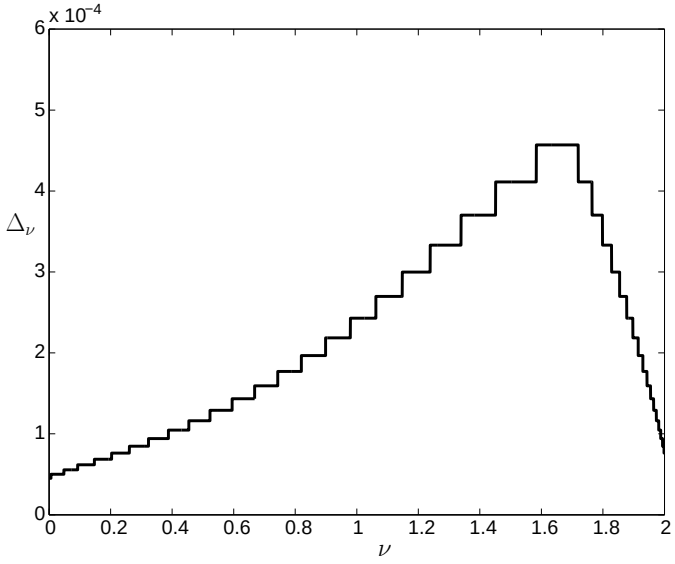

Figure 8: The step size Δ_ν as a function of the parameter $\nu \in [0, 2]$. The step size increases at first, but it then decreases as we approach a saddle-node bifurcation.

SH_rigorous_continuation(x_j,ν_j,ν_{j+1}) satisfy the geometric properties $\mathcal{H}$, as described in Section 4. Thus, the proof of Lemma 17 (and Lemma 22) was finished when all 60 runs ended successfully. The total running time was around 12 hours.

3.2 The bounds $Y_k(\Delta_\nu)$

Recalling (19) and (23), in this section we want to find bounds

$$\Big|[-A \cdot f(x_\nu, \nu)]_k\Big| \le Y_k(\Delta_\nu).$$

We use the following notation. For an arbitrary vector $y_F = (y_{-1}, y_0, y_1, \dots, y_{m-1})$ the infinite extension is $y = (y_{-1}, y_0, y_1, \dots, y_{m-1}, 0, 0, 0, \dots)$. For an infinite sequence $z = (z_{-1}, z_0, z_1, \dots)$, the finite restriction is $z_F = (z_{-1}, z_0, z_1, \dots, z_{m-1})$, whereas $z_I = (0, 0, \dots, 0, z_m, z_{m+1}, z_{m+2}, \dots)$ denotes the infinite tail. Similar notation is used for vectors/sequences of which the index starts at 0 rather than -1, in particular the vectors $\bar{a}_F = (\bar{a}_0, \bar{a}_1, \dots, \bar{a}_{m-1})$ and $\dot{a}_F = (\dot{a}_0, \dot{a}_1, \dots, \dot{a}_{m-1})$. Also, absolute values of vectors, infinite sequences, and matrices are taken component-wise, e.g., $|x| = (|x_{-1}|, |x_0|, |x_1|, |x_2|, \dots)$. Furthermore, we use the convolutions

$$(a * b * c)_k = \sum_{\substack{k_1+k_2+k_3=k \\ k_1,k_2,k_3 \in \mathbb{Z}}} a_{|k_1|} b_{|k_2|} c_{|k_3|},$$

which is of course the standard convolution when taking $a_{-k} \equiv a_k$, and (with the extension convention)

$$(a_F * b_F * c_F)_k = (a * b * c)_k = \sum_{\substack{k_1+k_2+k_3=k \\ |k_i|<m}} a_{|k_1|} b_{|k_2|} c_{|k_3|},$$

$k=-1$	
d^1_{-1}	$-2\bar{L}^2\sum_{l=1}^{m-1} l^2\dot{a}_l - 4\bar{L}\dot{L}\sum_{l=1}^{m-1} l^2\bar{a}_l - \sqrt{2}\left(\bar{a}_0 + 2\sum_{l=1}^{m-1}\bar{a}_l\right)\left(\dot{a}_0 + 2\sum_{l=1}^{m-1}\dot{a}_l\right)$
d^2_{-1}	$-4\bar{L}\dot{L}\sum_{l=1}^{m-1} l^2\dot{a}_l - 2\dot{L}^2\sum_{l=1}^{m-1} l^2\bar{a}_l - \frac{1}{2}\sqrt{2}\left(\dot{a}_0 + 2\sum_{l=1}^{m-1}\dot{a}_l\right)^2$
d^3_{-1}	$-2\dot{L}^2\sum_{l=1}^{m-1} l^2\dot{a}_l$
$k=0,1,2,\ldots$	
d^1_k	$\left(1+\nu_0\bar{L}^2k^2-\bar{L}^4k^4\right)\dot{a}_k + \left((2\nu_0\bar{L}\dot{L}+\bar{L}^2)k^2 - 4\bar{L}^3\dot{L}k^4\right)\bar{a}_k - 3(\bar{a}*\bar{a}*\dot{a})_k$
d^2_k	$\left((2\nu_0\bar{L}\dot{L}+\bar{L}^2)k^2 - 4\bar{L}^3\dot{L}k^4\right)\dot{a}_k + \left((\nu_0\dot{L}^2+2\bar{L}\dot{L})k^2 - 6\bar{L}^2\dot{L}^2k^4\right)\bar{a}_k - 3(\bar{a}*\dot{a}*\dot{a})_k$
d^3_k	$\left((\nu_0\dot{L}^2+2\bar{L}\dot{L})k^2 - 6\bar{L}^2\dot{L}^2k^4\right)\dot{a}_k + \left(\dot{L}^2k^2 - 4\bar{L}\dot{L}^3k^4\right)\bar{a}_k - (\dot{a}*\dot{a}*\dot{a})_k$
d^4_k	$\left(\dot{L}^2k^2 - 4\bar{L}\dot{L}^3k^4\right)\dot{a}_k - \dot{L}^4k^4\bar{a}_k$
d^5_k	$-\dot{L}^4k^4\dot{a}_k$

Table 1: The non-zero coefficients in the expansion (25) of f_k. In particular, $d^4_{-1} = d^5_{-1} = 0$. Notice that for $k \geq m$ the only non-vanishing terms are the convolution terms. Furthermore, for $k \geq 3m-2$ all coefficients are 0.

which vanishes for $k \geq 3m-2$.

Exploiting that f is a vector of polynomials in the components of x and ν, we write

$$f_k(x_\nu,\nu) = f_k(\bar{x}+\Delta_\nu\dot{x},\nu_0+\Delta_\nu) = f_k(\bar{x},\nu_0) + \sum_{i=1}^{5} d^i_k(\bar{x},\dot{x},\nu_0)\Delta^i_\nu. \tag{25}$$

Here the constants d^i_k are listed in Table 1. For the zeroth order term we have for the finite part $f_F(\bar{x},\nu_0) = f^{(m)}(\bar{x}_F,\nu_0)$, which is very small, since $\bar{x}_F$ is a numerical zero of $f^{(m)}(x_F,\nu_0)$. The choice of $\dot{x}_F$ given by (17) implies that the first order term d^1_F is also small, since

$$f_F(x_\nu,\nu) = f^{(m)}(\bar{x}_F,\nu_0) + \left[Df^{(m)}(\bar{x}_F,\nu_0)\dot{x}_F + \frac{\partial f}{\partial\nu}^{(m)}(\bar{x}_F,\nu_0)\right]\Delta_\nu + O(\Delta^2_\nu).$$

For the tail ($k \geq m$) we have $f_k(\bar{x},\nu_0) = -(\bar{a}*\bar{a}*\bar{a})_k = -(\bar{a}_F*\bar{a}_F*\bar{a}_F)_k$, which vanishes for $k \geq 3m-2$.

Using the vectors d^i from Table 1, this leads to bounds $Y_k(\Delta_\nu)$ as listed below, with $\Delta_\nu \geq 0$:

$$Y_F = |J_F\cdot f^{(m)}(\bar{x}_F,\nu_0)| + \sum_{i=1}^{5}\left|J_F\cdot d^i_F\right|\Delta^i_\nu, \tag{26a}$$

for $k=-1,0,1,\ldots,m-1$;

$$Y_k = \frac{|(\bar{a}*\bar{a}*\bar{a})_k| + 3|(\bar{a}*\bar{a}*\dot{a})_k|\Delta_\nu + 3|(\bar{a}*\dot{a}*\dot{a})_k|\Delta^2_\nu + |(\dot{a}*\dot{a}*\dot{a})_k|\Delta^3_\nu}{|\mu_k(\bar{L},\nu_0)|}, \tag{26b}$$

for $m \leq k \leq 3m-3$; and

$$Y_k = 0, \tag{26c}$$

for $k \geq 3m-2$.

3.3 The bounds $Z_k(r, \Delta_\nu)$

In this section we construct bounds

$$\sup_{w,w' \in W(r)} \Big| [DT_\nu(x_\nu + w')w]_k \Big| \le Z_k(r, \Delta_\nu).$$

We will use the notation introduced at the start of Section 3.2. Furthermore, at several instances, we employ a computational parameter M, and although not necessary, we choose the same value of M every time, for simplicity.

Recall that J_F is a numerical inverse of $Df^{(m)}(\bar{x}_F, \nu_0)$. To simplify the exposition, we introduce an almost inverse of the operator A defined in (18):

$$A^\dagger \stackrel{\text{def}}{=} \begin{bmatrix} Df^{(m)}(\bar{x}_F, \nu_0) & 0_F^T & 0_F^T & 0_F^T & \cdots \\ 0_F & \mu_m(\bar{L}, \nu_0) & 0 & 0 & \cdots \\ 0_F & 0 & \mu_{m+1}(\bar{L}, \nu_0) & 0 & \cdots \\ 0_F & 0 & 0 & \mu_{m+2}(\bar{L}, \nu_0) & \\ \vdots & \vdots & \vdots & & \ddots \end{bmatrix}.$$

We split $Df_\nu(x_\nu + w')w$ into two pieces:

$$Df_\nu(x_\nu + w')w = A^\dagger w + \big[Df_\nu(x_\nu + w') - A^\dagger\big]w,$$

hence

$$DT_\nu(w' + x_\nu)w = [I - AA^\dagger]w - A\,[Df_\nu(x_\nu + w') - A^\dagger]w, \tag{27}$$

where the first term will be very small. For $w, w' \in W(r)$ we consider $v, v' \in W(1)$ defined by $w = rv$ and $w' = rv'$. Similar to Section 3.2, we expand the expression $[Df_\nu(x_\nu + w') - A^\dagger]w$ in terms of r and Δ_ν:

$$\big([Df_\nu(x_\nu + w') - A^\dagger]w\big)_k = \sum_{i=1}^{5} \sum_{j=0}^{5-i} c_k^{i,j}(\bar{x}, \dot{x}, v, v', \nu_0) r^i \Delta_\nu^j, \tag{28}$$

Here the constants $c_k^{i,j}$ are listed in Table 2. Since $A^\dagger$ does not depend on r or Δ_ν, it is only involved in the calculation of the coefficient $c_k^{1,0}$. In particular, for the finite part

$$c_F^{1,0} = Df_F(\bar{x}, \nu_0)v - Df^{(m)}(\bar{x}_F, \nu_0)v_F,$$

and for the tail ($k \ge m$)

$$c_k^{1,0} = Df_k(\bar{x}, \nu_0)v - \mu_k(\bar{L}, \nu_0)v_k.$$

The other coefficients $c_k^{i,j}$ can be easily generated with the help of a computer (e.g. with Maple). Here we have rearranged the terms in the output somewhat, to make the formulas in Table 2 more aesthetically pleasing. However, such cosmetic changes are of course not needed for any *practical* purposes.

We now compute uniform upper bounds for the $c_k^{i,j}$, i.e., $C_k^{i,j} \ge 0$ such that

$$\Big| c_k^{i,j}(\bar{x}, \dot{x}, v, v', \nu_0) \Big| \le C_k^{i,j}(\bar{x}, \dot{x}, \nu_0), \qquad \text{for all } v, v' \in W(1). \tag{29}$$

The most involved are the convolution terms and we have a dedicated lemma to estimate those. Although the formulas are quite cumbersome, the numbers defined below

$k=-1$	
$c_{-1}^{1,0}$	$-2\bar{L}^2\sum_{l=m}^{\infty} l^2 v_l - \sqrt{2}\left(\bar{a}_0 + 2\sum_{l=1}^{m-1}\bar{a}_l\right)\left(2\sum_{l=m}^{\infty} v_l\right)$
$c_{-1}^{1,1}$	$-4\left(\dot{L}\sum_{l=1}^{m-1} l^2\bar{a}_l + \bar{L}\sum_{l=1}^{m-1} l^2\dot{a}_l\right)v_{-1} - 4\bar{L}\dot{L}\sum_{l=1}^{\infty} l^2 v_l - \sqrt{2}\left(\dot{a}_0 + 2\sum_{l=1}^{m-1}\dot{a}_l\right)\left(v_0 + 2\sum_{l=1}^{\infty} v_l\right)$
$c_{-1}^{1,2}$	$-4\dot{L}v_{-1}\sum_{l=1}^{m-1} l^2\dot{a}_l - 2\dot{L}^2\sum_{l=1}^{\infty} l^2 v_l$
$c_{-1}^{2,0}$	$-4\left(v'_{-1}\sum_{l=1}^{m-1} l^2\bar{a}_l + \bar{L}\sum_{l=1}^{\infty} l^2 v'_l\right)v_{-1} - 4\bar{L}v'_{-1}\sum_{l=1}^{\infty} l^2 v_l - \sqrt{2}\left(v'_0 + 2\sum_{l=1}^{\infty} v'_l\right)\left(v_0 + 2\sum_{l=1}^{\infty} v_l\right)$
$c_{-1}^{2,1}$	$-4\left(v'_{-1}\sum_{l=1}^{m-1} l^2\dot{a}_l + \dot{L}\sum_{l=1}^{\infty} l^2 v'_l\right)v_{-1} - 4\dot{L}v'_{-1}\sum_{l=1}^{\infty} l^2 v_l$
$c_{-1}^{3,0}$	$-4v'_{-1}v_{-1}\sum_{l=1}^{\infty} l^2 v'_l - 2(v'_{-1})^2\sum_{l=1}^{\infty} l^2 v_l$
$k=0,1,2,\dots$	
$c_k^{1,0}$	$\begin{cases} -3\,(\bar{a}*\bar{a}*v_I)_k & \text{for } 0\le k\le m-1 \\ -3\,(\bar{a}*\bar{a}*v)_k & \text{for } k\ge m \end{cases}$
$c_k^{1,1}$	$-k^2\left[\left(4k^2\bar{L}^3\dot{L} - \bar{L}^2 - 2\nu_0\bar{L}\dot{L}\right)v_k + 2\left((6k^2\bar{L}^2\dot{L} - \bar{L} - \nu_0\dot{L})\bar{a}_k + (2k^2\bar{L}^3 - \nu_0\bar{L})\dot{a}_k\right)v_{-1}\right] - 6\,(\bar{a}*\dot{a}*v)_k$
$c_k^{1,2}$	$-k^2\left[\left(6k^2\bar{L}^2\dot{L}^2 - 2\bar{L}\dot{L} - \nu_0\dot{L}^2\right)v_k + 2\left((6k^2\bar{L}\dot{L}^2 - \dot{L})\bar{a}_k + (6k^2\bar{L}^2\dot{L} - \bar{L} - \nu_0\dot{L})\dot{a}_k\right)v_{-1}\right] - 3\,(\dot{a}*\dot{a}*v)_k$
$c_k^{1,3}$	$-k^2\dot{L}\left[\left(4k^2\bar{L}\dot{L}^2 - \dot{L}\right)v_k + 2\left(2k^2\dot{L}^2\bar{a}_k + (6k^2\bar{L}\dot{L} - 1)\dot{a}_k\right)v_{-1}\right]$
$c_k^{1,4}$	$-k^4\dot{L}^3\left[\dot{L}v_k + 4\dot{a}_k v_{-1}\right]$
$c_k^{2,0}$	$-2k^2\left[\left(2k^2\bar{L}^3 - \nu_0\bar{L}\right)\left(v'_{-1}v_k + v'_k v_{-1}\right) + \left(6k^2\bar{L}^2 - \nu_0\right)\bar{a}_k v'_{-1}v_{-1}\right] - 6\,(\bar{a}*v'*v)_k$
$c_k^{2,1}$	$-2k^2\left[\left(6k^2\bar{L}^2\dot{L} - \bar{L} - \nu_0\dot{L}\right)\left(v'_{-1}v_k + v'_k v_{-1}\right) + \left((12k^2\bar{L}\dot{L} - 1)\bar{a}_k + (6k^2\bar{L}^2 - \nu_0)\dot{a}_k\right)v'_{-1}v_{-1}\right] - 6\,(\dot{a}*v'*v)_k$
$c_k^{2,2}$	$-2k^2\left[\left(6k^2\bar{L}\dot{L}^2 - \dot{L}\right)\left(v'_{-1}v_k + v'_k v_{-1}\right) + \left(6k^2\dot{L}^2\bar{a}_k + (12k^2\bar{L}\dot{L} - 1)\dot{a}_k\right)v'_{-1}v_{-1}\right]$
$c_k^{2,3}$	$-4k^4\dot{L}^2\left[\dot{L}\left(v'_{-1}v_k + v'_k v_{-1}\right) + 3\dot{a}_k v'_{-1}v_{-1}\right]$
$c_k^{3,0}$	$-k^2 v'_{-1}\left[\left(6k^2\bar{L}^2 - \nu_0\right)\left(v'_{-1}v_k + 2v'_k v_{-1}\right) + 12k^2\bar{L}\bar{a}_k v'_{-1}v_{-1}\right] - 3\,(v'*v'*v)_k$
$c_k^{3,1}$	$-k^2 v'_{-1}\left[\left(12k^2\bar{L}\dot{L} - 1\right)\left(v'_{-1}v_k + 2v'_k v_{-1}\right) + 12k^2\left(\dot{L}\bar{a}_k + \bar{L}\dot{a}_k\right)v'_{-1}v_{-1}\right]$
$c_k^{3,2}$	$-6k^4\dot{L}v'_{-1}\left[\dot{L}\left(v'_{-1}v_k + 2v'_k v_{-1}\right) + 2\dot{a}_k v'_{-1}v_{-1}\right]$
$c_k^{4,0}$	$-4k^4(v'_{-1})^2\left[\bar{L}\left(v'_{-1}v_k + 3v'_k v_{-1}\right) + \bar{a}_k v'_{-1}v_{-1}\right]$
$c_k^{4,1}$	$-4k^4(v'_{-1})^2\left[\dot{L}\left(v'_{-1}v_k + 3v'_k v_{-1}\right) + \dot{a}_k v'_{-1}v_{-1}\right]$
$c_k^{5,0}$	$-k^4(v'_{-1})^3\left[v'_{-1}v_k + 4v'_k v_{-1}\right]$

Table 2: The non-zero coefficients in the expansion (28). In the expression for $c_k^{1,0}$ we have used the notation $v_I = (0, 0, \dots, 0, v_m, v_{m+1}, v_{m+2}, \dots)$.

are easily calculated with a computer. We introduce the computational parameter $M \in \mathbb{N}$, arbitrary for now, and we define

$$\gamma_M \stackrel{\text{def}}{=} 2\left[\frac{M}{M-1}\right]^s + \left[\frac{4\ln(M-2)}{M} + \frac{\pi^2-6}{3}\right]\left[\frac{2}{M}+\frac{1}{2}\right]^{s_*-2},$$

where s_* is the largest integer such that $s_* \le s$, and

$$\beta_k \stackrel{\text{def}}{=} \begin{cases} 4 + \frac{1}{2^{2s-1}(2s-1)}, & k=0; \\ 2\left[2+\frac{1}{2^s}+\frac{1}{3^s}+\frac{1}{3^{s-1}(s-1)}\right] + \sum_{k_1=1}^{k-1} \frac{k^s}{k_1^s(k-k_1)^s}, & k=1,2,\dots,M-1; \\ 2\left[2+\frac{1}{2^s}+\frac{1}{3^s}+\frac{1}{3^{s-1}(s-1)}\right] + \gamma_M & k=M. \end{cases}$$

Using this, we set

$$\alpha_k = \frac{2\beta_M}{(M+k)^s(M-1)^{s-1}(s-1)} + \sum_{j=M}^{M+k-1} \frac{\beta_{j-k}}{j^s(j-k)^s}, \qquad \text{for } k=0,1,\dots,M-1,$$

while for $k=M$ we define

$$\alpha_M \stackrel{\text{def}}{=} \beta_0 + \sum_{j=1}^{M-1} \frac{\beta_j}{j^s}\left[1+\frac{1}{\left[1-\frac{j}{M}\right]^s}\right] + \beta_M\left[2+\frac{1}{2^s}+\frac{1}{3^s}+\frac{1}{3^{s-1}(s-1)}+\frac{1}{(M-1)^{s-1}(s-1)}+\gamma_M\right].$$

We introduce, for infinite sequence $a=(a_0,a_1,a_2,\dots)$, the notation

$$|a|_M = (|a|_0, |a|_1, \dots, |a|_{M-1}).$$

Analogous to (21) and (22), but now for sequences with index starting at 0 rather than -1, we define

$$\|a\|_s^0 \stackrel{\text{def}}{=} \sup_{k=0,1,\dots} |a_k\omega_k^s| = \sup\{|a_0|, |a_1|, 2^s|a_2|, 3^s|a_3|, 4^s|a_4|, \dots\},$$

and

$$W^0(r) \stackrel{\text{def}}{=} \{a\,,\, \|a\|_s^0 \le r\} = [-r,r] \times \prod_{k=1}^{\infty}\left[-\frac{r}{k^s}, \frac{r}{k^s}\right].$$

Lemma 18. *Let $M \ge 6$, and let a, b and c lie in the balls $W^0(A_a)$, $W^0(A_b)$ and $W^0(A_c)$. Then for $k=0,1,\dots,M-1$ we have*

$$(a*b*c)_k \;\in\; \left\{\left(|a|_M * |b|_M * |c|_M\right)_k + A_aA_bA_c\alpha_k\right\}[-1,1],$$

while for $k \ge M$ we have

$$(a*b*c)_k \;\in\; A_aA_bA_c\frac{\alpha_M}{k^s}\,[-1,1].$$

Proof. It is a special case of the general convolution estimates in Appendix A, with $p=3$, $M_1=M$, and the notation $\beta_k = \alpha_k^{(2)}$, $\alpha_k = \varepsilon_k^{(3)}$ and $\alpha_M = \alpha_M^{(3)}$. □

We are now ready to estimate the coefficients $c_k^{i,j}(\bar{x}, \dot{x}, v, v', \nu_0)$, but we first introduce a bit more notation, namely, in view of Lemma 18,

$$Q_k(a,b,c) \stackrel{\text{def}}{=} \begin{cases} \left(|a|_M * |b|_M * |c|_M\right)_k + \|a\|_s^0 \, \|b\|_s^0 \, \|c\|_s^0 \alpha_k, & k = 0, 1, \dots M-1; \\ \|a\|_s^0 \, \|b\|_s^0 \, \|c\|_s^0 \frac{\alpha_M}{k^s}, & k \geq M. \end{cases}$$

Furthermore, for $s > 1$, we use the notation

$$\zeta(s, l_0) \stackrel{\text{def}}{=} \sum_{l=l_0}^{\infty} \frac{1}{l^s}, \qquad \text{and} \qquad \zeta(s) \stackrel{\text{def}}{=} \zeta(s,1) = \sum_{l=1}^{\infty} \frac{1}{l^s},$$

and their estimates (which require only a finite computation), for $l_0 \leq M$,

$$\zeta_M(s, l_0) \stackrel{\text{def}}{=} \sum_{l=l_0}^{M} \frac{1}{l^s} + \frac{1}{(M-1)^{s-1}(s-1)}, \qquad \text{and} \qquad \zeta_M(s) \stackrel{\text{def}}{=} \zeta_M(s,1)$$

so that $\zeta(s, l_0) \leq \zeta_M(s, l_0)$ and $\zeta(s) \leq \zeta_M(s)$. Finally, let

$$\mathbb{I} \stackrel{\text{def}}{=} \left(1, 1, \frac{1}{2^s}, \frac{1}{3^s}, \frac{1}{4^s}, \cdots\right), \qquad \text{and} \qquad \mathbb{I}_I \stackrel{\text{def}}{=} \left(0, 0, \dots, 0, \frac{1}{m^s}, \frac{1}{(m+1)^s}, \dots\right).$$

With this notation in place, and using Lemma 18, the bounds $C_k^{i,j}(\bar{x}, \dot{x}, \nu_0)$ satisfying (29), listed in Table 3, are now straightforward to derive. For fixed k, these constants $C_k^{i,j}$ each only involve a finite computation, but there are of course still infinitely many values of k to consider. Notice first that for $k \geq m$ many terms in Table 3 vanish, since only the first m elements of $\bar{a}$ and $\dot{a}$ are nonzero. For the same reason, calculating $\|\bar{a}\|_s^0$ and $\|\dot{a}\|_s^0$ is a finite computation. Moreover, many terms can be estimated using the fact that, for any $A_1, A_2 \in \mathbb{R}$,

$$\left|A_1 + \frac{A_2}{k^2}\right| \leq \max\left\{\left|A_1 + \frac{A_2}{M^2}\right|, |A_1|\right\}, \qquad \text{for all } k \geq M.$$

It follows from these considerations and Lemma 18 that

$$C_k^{i,j} \leq \widehat{C}_M^{i,j} \, k^{4-s}, \qquad \text{for } k \geq M \geq \min\{m, 6\},$$

where the $\widehat{C}_M^{i,j}$ are listed in Table 4.

To conclude the calculation of Z_k we need an estimate on

$$|\mu_k(\bar{L}, \nu_0)| = \bar{L}^4 k^4 \left|1 - \frac{\nu_0}{\bar{L}^2 k^2} + \frac{1}{\bar{L}^4 k^4}\right|$$

for large k. Let

$$M_0(\bar{L}, \nu_0) \stackrel{\text{def}}{=} \begin{cases} 0 & \text{for } \nu_0 \leq 0, \\ \sqrt{2\nu_0}/\bar{L} & \text{for } \nu_0 > 0, \end{cases} \tag{30}$$

then it is not hard to check that

$$|\mu_k(\bar{L}, \nu_0)| \geq \frac{\bar{L}^4 k^4}{2} \qquad \text{for } k \geq M_0.$$

$k=-1$	
$C_{-1}^{1,0}$	$2\,\bar{L}^2\,\zeta_M(s-2,m)+2\sqrt{2}\,\Big\vert\bar{a}_0+2\sum_{l=1}^{m-1}\bar{a}_l\Big\vert\,\zeta_M(s,m)$
$C_{-1}^{1,1}$	$4\,\Big\vert\dot{L}\sum_{l=1}^{m-1}l^2\bar{a}_l+\bar{L}\sum_{l=1}^{m-1}l^2\dot{a}_l\Big\vert+4\big\vert\bar{L}\dot{L}\big\vert\,\zeta_M(s-2)+\sqrt{2}\,\Big\vert\dot{a}_0+2\sum_{l=1}^{m-1}\dot{a}_l\Big\vert\,\big[1+2\,\zeta_M(s)\big]$
$C_{-1}^{1,2}$	$4\,\Big\vert\dot{L}\sum_{l=1}^{m-1}l^2\dot{a}_l\Big\vert+2\dot{L}^2\,\zeta_M(s-2)$
$C_{-1}^{2,0}$	$8\big\vert\bar{L}\big\vert\,\zeta_M(s-2)+4\,\Big\vert\sum_{l=1}^{m-1}l^2\bar{a}_l\Big\vert+\sqrt{2}\,\big[1+2\,\zeta_M(s)\big]^2$
$C_{-1}^{2,1}$	$4\,\Big\vert\sum_{l=1}^{m-1}l^2\dot{a}_l\Big\vert+8\big\vert\dot{L}\big\vert\,\zeta_M(s-2)$
$C_{-1}^{3,0}$	$6\,\zeta_M(s-2)$
$k=0,1,2,\ldots$	
$C_k^{1,0}$	$\begin{cases}3\,Q_k(\bar{a},\bar{a},\mathbb{I}_I) & \text{for } 0\le k\le m-1\\ 3\,Q_k(\bar{a},\bar{a},\mathbb{I}) & \text{for } k\ge m\end{cases}$
$C_k^{1,1}$	$\Big\vert4k^2\bar{L}^3\dot{L}-\bar{L}^2-2\nu_0\bar{L}\dot{L}\Big\vert\,k^{2-s}+2\,\Big\vert2k^2\big(3\bar{L}^2\dot{L}\bar{a}_k+\bar{L}^3\dot{a}_k\big)-\big(\bar{L}\bar{a}_k+\nu_0\dot{L}\bar{a}_k+\nu_0\bar{L}\dot{a}_k\big)\Big\vert\,k^2+6\,Q_k(\bar{a},\dot{a},\mathbb{I})$
$C_k^{1,2}$	$\Big\vert6k^2\bar{L}^2\dot{L}^2-2\bar{L}\dot{L}-\nu_0\dot{L}^2\Big\vert\,k^{2-s}+2\,\Big\vert6k^2\big(\bar{L}\dot{L}^2\bar{a}_k+\bar{L}^2\dot{L}\dot{a}_k\big)-\big(\dot{L}\bar{a}_k+\bar{L}\dot{a}_k+\nu_0\dot{L}\dot{a}_k\big)\Big\vert\,k^2+3\,Q_k(\dot{a},\dot{a},\mathbb{I})$
$C_k^{1,3}$	$\Big\vert4k^2\bar{L}\dot{L}^3-\dot{L}^2\Big\vert\,k^{2-s}+2\,\Big\vert2k^2\big(\dot{L}^3\bar{a}_k+3\bar{L}\dot{L}^2\dot{a}_k\big)-\dot{L}\dot{a}_k\Big\vert\,k^2$
$C_k^{1,4}$	$\dot{L}^4k^{4-s}+4\big\vert\dot{L}^3\dot{a}_k\big\vert k^4$
$C_k^{2,0}$	$4\,\Big\vert2k^2\bar{L}^3-\nu_0\bar{L}\Big\vert\,k^{2-s}+2\,\Big\vert6k^2\bar{L}^2\bar{a}_k-\nu_0\bar{a}_k\Big\vert\,k^2+6\,Q_k(\bar{a},\mathbb{I},\mathbb{I})$
$C_k^{2,1}$	$4\,\Big\vert6k^2\bar{L}^2\dot{L}-\bar{L}-\nu_0\dot{L}\Big\vert\,k^{2-s}+2\,\Big\vert6k^2\big(2\bar{L}\dot{L}\bar{a}_k+\bar{L}^2\dot{a}_k\big)-\bar{a}_k-\nu_0\dot{a}_k\Big\vert\,k^2+6\,Q_k(\dot{a},\mathbb{I},\mathbb{I})$
$C_k^{2,2}$	$4\,\Big\vert6k^2\bar{L}\dot{L}^2-\dot{L}\Big\vert\,k^{2-s}+2\,\Big\vert6k^2\big(\dot{L}^2\bar{a}_k+2\bar{L}\dot{L}\dot{a}_k\big)-\dot{a}_k\Big\vert\,k^2$
$C_k^{2,3}$	$8\vert\dot{L}^3\vert k^{4-s}+12\dot{L}^2\vert\dot{a}_k\vert k^4$
$C_k^{3,0}$	$3\,\Big\vert6k^2\bar{L}^2-\nu_0\Big\vert\,k^{2-s}+12\big\vert\bar{L}\bar{a}_k\big\vert k^4+3\,Q_k(\mathbb{I},\mathbb{I},\mathbb{I})$
$C_k^{3,1}$	$3\,\Big\vert12k^2\bar{L}\dot{L}-1\Big\vert\,k^{2-s}+12\,\Big\vert\dot{L}\bar{a}_k+\bar{L}\dot{a}_k\Big\vert\,k^4$
$C_k^{3,2}$	$18\dot{L}^2k^{4-s}+12\big\vert\dot{L}\dot{a}_k\big\vert k^4$
$C_k^{4,0}$	$16\big\vert\bar{L}\big\vert k^{4-s}+4\vert\bar{a}_k\vert k^4$
$C_k^{4,1}$	$16\big\vert\dot{L}\big\vert k^{4-s}+4\vert\dot{a}_k\vert k^4$
$C_k^{5,0}$	$5\,k^{4-s}$

Table 3: The bounds uniform $C_k^{i,j}(\bar{x},\dot{x},\nu_0)$ on the coefficients $c_k^{i,j}(\bar{x},\dot{x},v,v',\nu_0)$. For $k=0$ one should read $k^{2-s}=0$ and $k^{4-s}=0$, irrespective of s.

$\widehat{C}_M^{1,0}$	$\frac{3(\|\bar{a}\|_s^0)^2\alpha_M}{M^4}$
$\widehat{C}_M^{1,1}$	$\max\left\{\left\|4\bar{L}^3\dot{L}-\frac{\bar{L}^2+2\nu_0\bar{L}\dot{L}}{M^2}\right\|,4\left\|\bar{L}^3\dot{L}\right\|\right\}+\frac{6\|\bar{a}\|_s^0\|\dot{a}\|_s^0\alpha_M}{M^4}$
$\widehat{C}_M^{1,2}$	$\max\left\{\left\|6\bar{L}^2\dot{L}^2-\frac{2\bar{L}\dot{L}+\nu_0\dot{L}^2}{M^2}\right\|,6\bar{L}^2\dot{L}^2\right\}+\frac{3(\|\dot{a}\|_s^0)^2\alpha_M}{M^4}$
$\widehat{C}_M^{1,3}$	$\max\left\{\left\|4\bar{L}\dot{L}^3-\frac{\dot{L}^2}{M^2}\right\|,4\left\|\bar{L}\dot{L}^3\right\|\right\}$
$\widehat{C}_M^{1,4}$	$\dot{L}^4$
$\widehat{C}_M^{2,0}$	$4\max\left\{\left\|2\bar{L}^3-\frac{\nu_0\bar{L}}{M^2}\right\|,2\left\|\bar{L}^3\right\|\right\}+\frac{6\|\bar{a}\|_s^0\alpha_M}{M^4}$
$\widehat{C}_M^{2,1}$	$4\max\left\{\left\|6\bar{L}^2\dot{L}-\frac{\bar{L}+\nu_0\dot{L}}{M^2}\right\|,6\bar{L}^2\left\|\dot{L}\right\|\right\}+\frac{6\|\dot{a}\|_s^0\alpha_M}{M^4}$
$\widehat{C}_M^{2,2}$	$4\max\left\{\left\|6\bar{L}\dot{L}^2-\frac{\dot{L}}{M^2}\right\|,6\left\|\bar{L}\right\|\dot{L}^2\right\}$
$\widehat{C}_M^{2,3}$	$8\left\|\dot{L}^3\right\|$
$\widehat{C}_M^{3,0}$	$3\max\left\{\left\|6\bar{L}^2-\frac{\nu_0}{M^2}\right\|,6\bar{L}^2\right\}+\frac{3\alpha_M}{M^4}$
$\widehat{C}_M^{3,1}$	$3\max\left\{\left\|12\bar{L}\dot{L}-\frac{1}{M^2}\right\|,12\left\|\bar{L}\dot{L}\right\|\right\}$
$\widehat{C}_M^{3,2}$	$18\dot{L}^2$
$\widehat{C}_M^{4,0}$	$16\left\|\bar{L}\right\|$
$\widehat{C}_M^{4,1}$	$16\left\|\dot{L}\right\|$
$\widehat{C}_M^{5,0}$	5

Table 4: The uniform bounds $\widehat{C}_M^{i,j}$ on $k^{s-4}C_k^{i,j}(\bar{x},\dot{x},\nu_0)$ for $k\geq M$.

Using the vectors $C^{i,j}$ and the numbers $\widehat{C}_M^{i,j}$ from Tables 3 and 4, and in view of (27), this leads to bounds $Z_k(r, \Delta_\nu)$ as listed below, with $M \geq \min\{M_0, m, 6\}$ and $\Delta_\nu \geq 0$:

$$Z_F = |I - J_F \cdot Df^{(m)}(\bar{x}_F, \nu_0)| \cdot \mathbb{I}_F \, r + \sum_{i=1}^{5} \sum_{j=0}^{5-i} \big|J_F\big| \cdot C_F^{i,j} \, r^i \, \Delta_\nu^j, \tag{31a}$$

for $k = -1, 0, 1, \ldots, m-1$;

$$Z_k = \frac{1}{|\mu_k(\bar{L}, \nu_0)|} \sum_{i=1}^{5} \sum_{j=0}^{5-i} C_k^{i,j} \, r^i \, \Delta_\nu^j, \tag{31b}$$

for $m \leq k \leq M-1$; and

$$Z_k = \frac{2}{\bar{L}^4} \frac{1}{k^s} \sum_{i=1}^{5} \sum_{j=0}^{5-i} \widehat{C}_M^{i,j} \, r^i \, \Delta_\nu^j, \tag{31c}$$

for $k \geq M$. Finally, for the purpose of Definition 14 and Lemma 15, we set

$$\widehat{Z}_M \stackrel{\text{def}}{=} \frac{2}{\bar{L}^4 M^s} \sum_{i=1}^{5} \sum_{j=0}^{5-i} \widehat{C}_M^{i,j} \, r^i \, \Delta_\nu^j, \tag{32}$$

so that $Z_k = \widehat{Z}_M \big(\frac{M}{k}\big)^s$.

4 Verification of the Geometric Properties $\mathcal{H}$

We now put ourselves in the situation of a single, successful, rigorous continuation step, where we have found an $r > 0$ such that the set ($s > 3$)

$$W_{x_\nu}(r) = x_\nu + W(r), \qquad \text{with } x_\nu = \bar{x} + (\nu - \nu_0)\dot{x}, \tag{33}$$

centered at the predictor based at ν_0, contains a unique fixed point $\widetilde{x}^\nu$ of $T(x, \nu)$ for each parameter value $\nu \in [\nu_0, \nu_1]$. We write $\widetilde{x}^\nu = (\widetilde{L}^\nu, \widetilde{a}_0^\nu, \widetilde{a}_1^\nu, \widetilde{a}_2^\nu, \ldots)$. The functions $\widetilde{u}^\nu$ defined via (11), are periodic solutions of (4) with period $2\pi/\widetilde{L}^\nu$, which are symmetric in $y = 0$ and $y = \pi/\widetilde{L}^\nu$. For convenience, we incorporate the period of the periodic solution in the definition of the geometric condition as follows:

$$\mathcal{H}_{\widetilde{L}} \begin{cases} (H_1) & \widetilde{u} \text{ has exactly four monotone laps and extrema } \{\widetilde{u}_i\}_{i=1}^4 \text{ on } [0, 2\pi/\widetilde{L}]; \\ (H_2) & \widetilde{u}_1 \text{ and } \widetilde{u}_3 \text{ are minima, and } \widetilde{u}_2 \text{ and } \widetilde{u}_4 \text{ are maxima;} \\ (H_3) & \widetilde{u}_1 < -1 < \widetilde{u}_3 < 1 < \widetilde{u}_2, \widetilde{u}_4; \\ (H_4) & \widetilde{u}(x) \text{ is symmetric in its minima } \widetilde{u}_1 \text{ and } \widetilde{u}_3. \end{cases}$$

We need to make sure that the unique zero of f in W_{x_ν} satisfies these properties. The following lemma will help us in the verification process, since it shows that we only need to check the conditions for *one* parameter value along any continuous branch of solutions.

Lemma 19. *Let $\widetilde{u}^\nu$, $\nu_0 \leq \nu \leq \nu_1$ be periodic solutions of (4) at the energy level $E = 0$ with period $2\pi/\widetilde{L}^\nu$, which are symmetric in $y = 0$ and $y = \pi/\widetilde{L}^\nu$. Suppose that $\widetilde{u}^\nu$ and $\widetilde{L}^\nu$ depend continuously on ν, i.e., $\widetilde{u}^\nu$ depends continuously on ν as a C^3-function on compact intervals. If $\widetilde{u}^{\nu_0}$ satisfies $\mathcal{H}_{\widetilde{L}^{\nu_0}}$, then $\widetilde{u}^\nu$ satisfies $\mathcal{H}_{\widetilde{L}^\nu}$ for all $\nu \in [\nu_0, \nu_1]$.*

Proof. To reduce clutter, we remove all tildes from the notation. By symmetry, we only need to consider the interval $[0, \pi/L^\nu]$. Let

$$N = \left\{ \nu \in [\nu_0, \nu_1] \;\middle|\; u^\nu \text{ satisfies } \mathcal{H}_{L^\nu} \right\}.$$

By assumption, $\nu_0 \in N$. We will show that N is both open and closed (in the relative topology), i.e. connected, hence $N = [\nu_0, \nu_1]$ as asserted.

It is relatively easy to see that N is open. Namely, for $\nu \in N$ the extrema of u^ν do not lie on the lines $u = \pm 1$. It then follows from the energy identity $E = 0$ that the extrema of u^ν are all non-degenerate. Hence, the conditions $H_{1,2,3,4}$ are open conditions (under the symmetry assumption in the lemma).

To prove that N is closed, is a bit more involved. Let $\{\nu_n\}_{n=1}^\infty \subset N$ be a sequence converging to $\nu_* \in [\nu_0, \nu_1]$. Our goal is to show that $\nu_* \in N$. We denote $u^n = u^{\nu_n}$ and $u_* = u^{\nu_*}$. Let the extrema $u^n_{1,2,3}$ be attained in $y^n_{1,2,3}$. Clearly, we have that $y^n_1 = 0$ and $y^n_3 = \pi/L^\nu_n$, while, taking a subsequence, we may additionally assume that y^n_2 converges to some y^*_2 as $n \to \infty$. Denote also $y^*_1 = 0$ and $y^*_3 = \pi/L^{\nu_*}$. By C^3-continuity, we have $u'_*(y^*_{1,2,3}) = 0$, and

$$u_*(y^*_1) \le -1 \le u_*(y^*_3) \le 1 \le u_*(y^*_2). \tag{34}$$

In fact, the inequalities are strict. We prove this for the last inequality $u_*(y^*_2) > 1$; the other cases are analogous. Suppose, by contradiction, that $u_*(y^*_2) = 1$. Since $u'_*(y^*_2) = 0$, it follows from $E = 0$ that $u''_*(y^*_2) = 0$. By continuity,

$$\max_y u_*(y) = \lim_{n\to\infty} \max_y u^n(y) = \lim_{n\to\infty} u^n(y^n_2) = u_*(y^*_2) = 1.$$

This implies that $u'''_*(y^*_2) = 0$. Uniqueness of the initial value problem for the ODE then says that $u_*(y) = 1$ for all y, which contradicts $u_*(y^*_1) \le -1$. Similarly one can show that all the other inequalities in (34) are strict, hence u_* has at least four extrema on $[0, 2\pi/L^{\nu_*}]$, and those satisfy H_3.

The final step is to prove that u_* does not have more than four monotone laps. We argue once more by contradiction. Recall that $y^*_2 = \lim_{n\to\infty} y^n_2$. Suppose there is a point $z \in (0, \pi/L^{\nu_*})$ with $u'_*(z) = 0$, and $z \neq y^*_2$. If $u''_*(z) \neq 0$, then, by the implicit function theorem, this extremum persists for u^n for n sufficiently large, leading to more than four monotone laps of u^n, contradicting the fact that u^n satisfies the geometric conditions. Hence, it must be that $u''_*(z) = 0$, and thus $u_*(z) = \pm 1$, since $E = 0$. Moreover, since $u_* \not\equiv \pm 1$, we must have $u'''_*(z) \neq 0$. Let us consider the case $u_*(z) = 1$ and $u'''_*(z) > 0$; all other (three) cases are analogous.

We thus have

$$u_*(z) = 1, \quad u'_*(z) = 0, \quad u''_*(z) = 0, \quad u'''_*(z) > 0. \tag{35}$$

Clearly $u'_*(y) > 0$ for y sufficiently close but not equal to z. By continuity, we have $(u^n)'(z \pm \varepsilon) > 0$ for ε sufficiently small and n large enough. By the implicit function theorem, for large enough n, there exist points $z_n \in [z - \varepsilon, z + \varepsilon]$ such that $\lim_{n\to\infty} z_n = z$ and $(u^n)''(z_n) = 0$, and $(u^n)'(z_n) \neq 0$, since u^n has no additional extrema in $(0, L^{\nu_n})$ besides y^n_2. In fact, $(u^n)'(z_n) > 0$, since if $(u^n)'(z_n) < 0$ then u^n would have two extrema in $[z - \varepsilon, z + \varepsilon]$, leading to more than four monotone laps of u^n, a contradiction. Hence $(u^n)'(z_n) > 0$.

We conclude from $E = 0$ and $(u^n)''(z_n) = 0$ that

$$\Big[(u^n)'''(z_n) + \frac{\nu_n}{2}(u^n)'(z_n)\Big](u^n)'(z_n) = -\frac{1}{4}(u^n(z_n)^2 - 1)^2.$$

Since $(u^n)'(z_n) > 0$, this means that

$$(u^n)'''(z_n) + \frac{\nu_n}{2}(u^n)'(z_n) \leq 0.$$

Finally, we take the limit $n \to \infty$ in the above inequality to obtain

$$u_*'''(z) + \frac{\nu_*}{2}u_*'(z) \leq 0,$$

which contradicts (35). Hence u_* indeed has exactly four monotone laps on $[0, 2\pi/L^{\nu_*}]$, implying that $\nu_* \in N$ and that N is closed. □

We now only need to show that the geometric properties are satisfied at $\nu = \nu_0$, since the solutions depends continuously on ν.

Lemma 20. *The fixed point $\widetilde{x}_\nu \in \Omega^s$ depends continuously on ν for $\nu \in [\nu_0, \nu_1]$. Similarly, the corresponding periodic solutions $\widetilde{u}_\nu$ depend continuously on ν as C^3-functions on compact intervals.*

Proof. Recall that we are dealing with a single continuation step $\nu \in [\nu_0, \nu_1]$, so that the neighborhoods on which T is a contraction mapping are given by (33). The assertion now follows from the continuity and compactness properties of the map T, described in Lemma 12, using standard functional analytic arguments. □

To check that $\widetilde{u}^{\nu_0}$ has the properties $\mathcal{H}_{\widetilde{L}^{\nu_0}}$, we follow the procedure outlined below. To reduce clutter, we often drop ν_0 from the notation. We introduce the variables $z = \widetilde{L}^{\nu_0} y$ and $v(z) = \widetilde{u}^{\nu_0}(y)$, so that

$$v(z) = \widetilde{a}_0 + 2\sum_{k=1}^{\infty} \widetilde{a}_k \cos(kz).$$

This way, we separate the shape of the solution from the period; only the shape is important for the geometric conditions. Clearly, $v'(0) = v'(\pi) = 0$, and v is symmetric in those extrema.

We recall that $\bar{x} = (\bar{L}, \bar{a}_0, \bar{a}_1, \dots, \bar{a}_{m-1}, 0, 0, \dots)$, while the fixed point is given by $\widetilde{x} = (\widetilde{L}, \widetilde{a}_0, \widetilde{a}_1, \widetilde{a}_2, \dots)$. We have $\widetilde{a}_k \in \mathbf{a}_k$, where the intervals are given by

$$\mathbf{a}_k \stackrel{\text{def}}{=} \begin{cases} [\bar{a}_0 - r, \bar{a}_0 + r], & k = 0; \\ [\bar{a}_k - \frac{r}{k^s}, \bar{a}_k + \frac{r}{k^s}], & k = 1, \dots, m-1; \\ [-\frac{r}{k^s}, \frac{r}{k^s}], & k \geq m. \end{cases}$$

Consider $z \in \mathbf{z} \stackrel{\text{def}}{=} [z^-, z^+] \subset \mathbb{R}$. Then, using interval arithmetic, we can compute rigorous interval enclosures of $v(z)$, $v'(z)$ and $v''(z)$:

$$v(z) \in \quad \mathbf{v}[\mathbf{z}] \stackrel{\text{def}}{=} \mathbf{a}_0 + 2\sum_{k=1}^{m-1} \mathbf{a}_k \cos(k\mathbf{z}) + \frac{2r}{(m-1)^{s-1}(s-1)}[-1,1],$$

$$v'(z) \in \ \mathbf{v}'[\mathbf{z}] \stackrel{\text{def}}{=} -2\sum_{k=1}^{m-1} \mathbf{a}_k\, k \sin(k\mathbf{z}) + \frac{2r}{(m-1)^{s-2}(s-2)}[-1,1],$$

$$v''(z) \in \mathbf{v}''[\mathbf{z}] \stackrel{\text{def}}{=} -2\sum_{k=1}^{m-1} \mathbf{a}_k\, k^2 \cos(k\mathbf{z}) + \frac{2r}{(m-1)^{s-3}(s-3)}[-1,1].$$

We now use the following procedure, see also Figure 9. Note that we know a priori that $v'(0) = v'(\pi) = 0$.

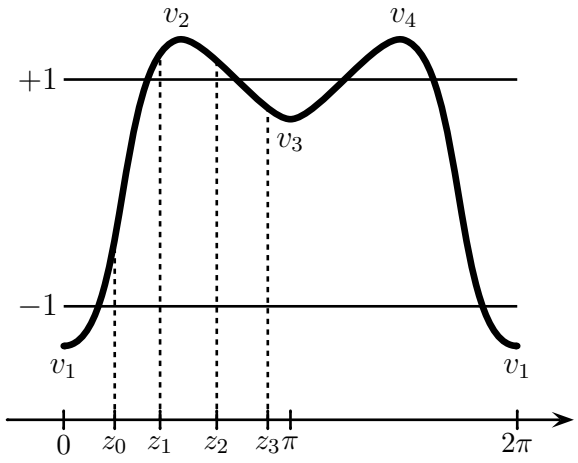

Figure 9: Illustration of the procedure to make sure that v satisfies $\mathcal{H}_\pi$, i.e., the periodic solution $\widetilde{u}^{\nu_0}$ satisfies the geometric conditions $\mathcal{H}_{\widetilde{L}_0^\nu}$. The extrema are denoted by $v_i = \widetilde{u}_i^{\nu_0}$.

Procedure 21. *Checking that $\widetilde{u}^{\nu_0}$ satisfies $\mathcal{H}_{\widetilde{L}^{\nu_0}}$ is equivalent to verifying that v satisfies $\mathcal{H}_\pi$. We proceed as follows.*

1. *Verify that $\mathbf{v}[0] \subset (-\infty, -1)$. That implies that $\widetilde{u}_1^{\nu_0} = v(0) < -1$.*
2. *Find an (approximately largest) $z_0 > 0$ such that $\mathbf{v}''[0, z_0] \subset (0, \infty)$. Hence, there is a unique extremum in $[0, z_0]$, namely a minimum, at $z = 0$.*
3. *Find an (approximately largest) $z_1 > z_0$ such that $\mathbf{v}'[z_0, z_1] \subset (0, \infty)$. Hence, the interval $[z_0, z_1]$ does not contain any extremum.*
4. *Verify that $\mathbf{v}[z_1] \subset (1, \infty)$.*
5. *Find an (approximately largest) $z_2 > z_1$ such that both $\mathbf{v}[z_1, z_2] \subset (1, \infty)$ and $\mathbf{v}''[z_1, z_2] \subset (-\infty, 0)$.*
6. *Verify that $\mathbf{v}'[z_2] \subset (-\infty, 0)$. That implies that there is a unique extremum z_* in $[z_1, z_2]$, namely a maximum $\widetilde{u}_2^{\nu_0} = v(z_*) > 1$.*
7. *Find an (approximately largest) $z_3 > z_2$ such that $\mathbf{v}'[z_2, z_3] \subset (-\infty, 0)$. Hence, the interval $[z_2, z_3]$ does not contain any extremum.*
8. *Verify that $\mathbf{v}''[z_3, \pi] \subset (0, \infty)$ and $\mathbf{v}[\pi] \subset (-1, 1)$. That implies that there is a unique extremum in $[z_3, \pi]$, namely a minimum $\widetilde{u}_3^{\nu_0} = v(\pi) \in (-1, 1)$ at $z = \pi$.*

Combining Lemma 19 with Procedure 21 leads to the required result.

Lemma 22. *The choice of the approximate zero $\widehat{x}_F^*$ of $f^{(m)}(x_F, 0)$ in Lemma 17 can be made such that for each of the resulting intervals $[\nu_0, \nu_0 + \Delta_\nu^0]$ covering $[0, 2]$, which were extracted in Procedure 16, the Procedure 21 is successful at ν_0. Hence the solutions found in Lemma 17 via Procedure 16 satisfy the geometric conditions $\mathcal{H}$.*

The movie *SH_geometry_movie.mp4*, accompanying this paper, shows the changing shape of the periodic solution $\widetilde{u}^\nu$ as the parameter ν increases from 0 to 2.

Proof. A *Matlab* computer program (*SH_geometric_properties.m*, see also Section 3.1) successfully performing Procedure 21 accompanies the paper. The numerical implementation of Procedure 21 is rather straightforward. Steps 1, 4, 6 and the second part of Step 8 are mere evaluations of a function using interval arithmetic. Steps 2, 3, 5, 7 and the first part of Step 8 are all implemented in the same fashion. For instance, we describe here what is done in the implementation of Step 3. First, we consider a mesh $\{x_0, \dots, x_n\}$ of the interval $[z_0, \pi]$ and we find the largest $k \in \{1, \dots, n\}$ for which we have that $\mathbf{v}'[x_{i-1}, x_i] \subset (1, \infty)$, for all $i \in \{1, \dots, k\}$. We then let $z_1 = x_i$. Note that the smaller the mesh size, the nearer z_1 will be to a zero of v'. Every verification thus requires a series of evaluations of $\mathbf{v}$, $\mathbf{v}'$ and $\mathbf{v}''$ using interval arithmetic. In the implementation, we chose the mesh size to be 0.01. □

In conclusion, Theorem 3 is a consequence of Lemmas 17 and 22, which are based on Procedures 16 and 21, respectively.

Appendix A: Estimates for infinite convolution sums with power decay

In this section, we present two lemmas that are fundamental in the construction of the radii polynomials. Let $s \geq 2$ be a real number and $M \geq 6$ a natural number.

We introduce an improvement of general estimates for infinite convolution sums with power decay of the form

$$\sum_{k_1+\cdots+k_p=k} a^{(1)}_{k_1} \cdots a^{(p)}_{k_p}, \tag{36}$$

introduced in [11, 13] and used in [12, 14, 17]. Most of the estimates used in the above papers are corollaries of Lemma 5.8 in [13]:

Lemma 23 (from [13])**.** *Let $A > 0$ and $s \geq 2$. Let $\{a_k\}_{k\in\mathbb{Z}}$ be such that $a_{-k} = a_k$, $a_0 \in A[-1, 1]$ and $a_k \in \frac{A}{|k|^s}$ for all $k \in \mathbb{Z} \setminus \{0\}$. Let $\alpha = \frac{2}{s-1} + 2 + 3.5 \cdot 2^s$. Then*

$$\sum_{\sum n_i = k} a_{n_1} \cdots a_{n_p} \subseteq \begin{cases} \alpha^{p-1} A^p [-1, 1] & k = 0, \\ \frac{\alpha^{p-1} A^p}{|k|^s} [-1, 1] & k \neq 0. \end{cases}$$

Observe that the coefficient α provided by Lemma 23 grows exponentially in s. One reason for being interested in getting tighter analytic estimates for sums of the form (36), comes from the fact that in solving equations (13) and (14), we need $p = 3$ and $s \geq 4$. If we use the bounds given by Lemma 23, the computational cost of the rigorous continuation will dramatically increase, since we will need to use a very large computational parameter M. A lower bound on M (depending on the α of Lemma 23) can actually be found in ([17], Section 2.2).

In this appendix we consider general values of the degree p of the convolution and the decay power s, since the specific case is hardly any simpler than the general one. Moreover, the general convolution estimates may be of use for future applications of the method laid out in this paper.

Throughout this appendix we assume that $a_{-k} = a_k$ for all $k \in \mathbb{Z}$. Since

$$\sum_{\substack{k_1+\cdots+k_p=-k \\ k_i\in\mathbb{Z}}} a^{(1)}_{k_1}\cdots a^{(p)}_{k_p} = \sum_{\substack{k_1+\cdots+k_p=k \\ k_i\in\mathbb{Z}}} a^{(1)}_{k_1}\cdots a^{(p)}_{k_p}\,,$$

we only consider the cases $k \in \mathbb{N}$. Note that the estimates are also applicable to the situation where $a_{-k} = -a_k$ for all k.

Before introducing the new general estimates, we need the following result.

Lemma 24. *Let $s \geq 2$ and let s_* be the largest integer such that $s_* \leq s$. Let, for $k \geq 4$,*

$$\gamma_k \stackrel{\text{def}}{=} 2\left[\frac{k}{k-1}\right]^s + \left[\frac{4\ln(k-2)}{k} + \frac{\pi^2-6}{3}\right]\left[\frac{2}{k}+\frac{1}{2}\right]^{s_*-2}. \tag{37}$$

Then, for $k \geq 4$,

$$\sum_{k_1=1}^{k-1} \frac{k^s}{k_1^s(k-k_1)^s} \leq \gamma_k\,.$$

Proof. First observe that

$$\begin{aligned}
\sum_{k_1=1}^{k-1} \frac{k^s}{k_1^s(k-k_1)^s} &= 2\left[\frac{k}{k-1}\right]^s + \sum_{k_1=2}^{k-2} \frac{k^s}{k_1^s(k-k_1)^s} \\
&= 2\left[\frac{k}{k-1}\right]^s + k^{s-1}\sum_{k_1=2}^{k-2} \frac{(k-k_1)+k_1}{k_1^s(k-k_1)^s} \\
&= 2\left[\frac{k}{k-1}\right]^s + k^{s-1}\left[\sum_{k_1=2}^{k-2} \frac{1}{k_1^s(k-k_1)^{s-1}} + \sum_{k_1=2}^{k-2} \frac{1}{k_1^{s-1}(k-k_1)^s}\right] \\
&= 2\left[\frac{k}{k-1}\right]^s + 2\sum_{k_1=2}^{k-2} \frac{k^{s-1}}{k_1^{s-1}(k-k_1)^s}\,.
\end{aligned}$$

We now set, using the above,

$$\begin{aligned}
\phi_k^{(s)} &\stackrel{\text{def}}{=} \sum_{k_1=2}^{k-2} \frac{k^{s-1}}{k_1^{s-1}(k-k_1)^s} \\
&= \frac{1}{2}\sum_{k_1=2}^{k-2} \frac{k^s}{k_1^s(k-k_1)^s}.
\end{aligned}$$

We now obtain the recurrence inequality

$$\begin{aligned}
\phi_k^{(s)} &= \sum_{k_1=2}^{k-2} \frac{k^{s-1}}{k_1^{s-1}(k-k_1)^s} = k^{s-2} \sum_{k_1=2}^{k-2} \frac{(k-k_1)+k_1}{k_1^{s-1}(k-k_1)^s} \\
&= k^{s-2} \left[\sum_{k_1=2}^{k-2} \frac{1}{k_1^{s-1}(k-k_1)^{s-1}} + \sum_{k_1=2}^{k-2} \frac{1}{k_1^{s-2}(k-k_1)^s} \right] \\
&= \frac{1}{k} \sum_{k_1=2}^{k-2} \frac{k^{s-1}}{k_1^{s-1}(k-k_1)^{s-1}} + \sum_{k_1=2}^{k-2} \frac{k^{s-2}}{k_1^{s-2}(k-k_1)^s} \\
&\leq \frac{1}{k} \sum_{k_1=2}^{k-2} \frac{k^{s-1}}{k_1^{s-1}(k-k_1)^{s-1}} + \frac{1}{2} \sum_{k_1=2}^{k-2} \frac{k^{s-2}}{k_1^{s-2}(k-k_1)^{s-1}} \\
&= \left[\frac{2}{k} + \frac{1}{2} \right] \phi_k^{(s-1)}.
\end{aligned}$$

Hence, since $\frac{k}{k_1(k-k_1)} \leq 1$ for $2 \leq k_1 \leq k-2$ and $k \geq 4$,

$$\phi_k^{(s)} \leq \phi_k^{(s_*)} \leq \phi_k^{(2)} \left[\frac{2}{k} + \frac{1}{2} \right]^{s_*-2},$$

where s_* is the largest integer such that $s_* \leq s$, and

$$\begin{aligned}
\phi_k^{(2)} &= \sum_{k_1=2}^{k-2} \frac{k}{k_1(k-k_1)^2} = \sum_{k_1=2}^{k-2} \frac{1}{k_1(k-k_1)} + \sum_{k_1=2}^{k-2} \frac{1}{(k-k_1)^2} \\
&= \frac{2}{k} \sum_{k_1=2}^{k-2} \frac{1}{k_1} + \sum_{k_1=2}^{k-2} \frac{1}{k_1^2} \;\leq\; \frac{2}{k} \ln(k-2) + \frac{\pi^2}{6} - 1\,.
\end{aligned}$$

By combining the above inequalities, we conclude that

$$\sum_{k_1=1}^{k-1} \frac{k^s}{k_1^s(k-k_1)^s} \leq 2 \left[\frac{k}{k-1} \right]^s + \left[\frac{4\ln(k-2)}{k} + \frac{\pi^2-6}{3} \right] \left[\frac{2}{k} + \frac{1}{2} \right]^{s_*-2} = \gamma_k. \qquad \square$$

Note that the estimates will be given via a recurrent definition in p, i.e., the power of the nonlinearity. Hence, we begin by getting explicitly the estimates for the case $p = 2$. Throughout this note, we use $M \geq 6$ as a computational parameter; its use is primarily to make all the estimates computable in practice.

A.1 Estimates for the quadratic nonlinearity

Lemma 25 (Quadratic Estimates)**.** *Let $s \geq 2$ and $M \geq 6$. Define*

$$\alpha_k^{(2)} \stackrel{\text{def}}{=} \begin{cases} 4 + \frac{1}{2^{2s-1}(2s-1)} & \text{for } k = 0, \\ 2\left[2 + \frac{1}{2^s} + \frac{1}{3^s} + \frac{1}{3^{s-1}(s-1)}\right] + \sum_{k_1=1}^{k-1} \frac{k^s}{k_1^s(k-k_1)^s} & \text{for } 1 \leq k \leq M-1, \\ 2\left[2 + \frac{1}{2^s} + \frac{1}{3^s} + \frac{1}{3^{s-1}(s-1)}\right] + \gamma_k & \text{for } k \geq M. \end{cases}$$

Let $A_1, A_2 > 0$ such that $a_0^{(i)} \in A_i[-1,1]$ and $a_k^{(i)} \in \frac{A_i}{|k|^s}[-1,1]$, for all $k \neq 0$ and for $i = 1, 2$. Suppose that $a_{-k}^{(i)} = a_k^{(i)}$. Then

$$\sum_{\substack{k_1+k_2=k \\ k_i \in \mathbb{Z}}} a_{k_1}^{(1)} a_{k_2}^{(2)} \in \begin{cases} \alpha_0^{(2)} A_1 A_2 \, [-1,1] & k = 0, \\ \frac{\alpha_k^{(2)} A_1 A_2}{|k|^s} \, [-1,1] & k \neq 0. \end{cases}$$

Proof. Let $k = 0$. Then

$$\begin{aligned} \sum_{\substack{k_1+k_2=0 \\ k_i \in \mathbb{Z}}} a_{k_1}^{(1)} a_{k_2}^{(2)} &= \sum_{k_1<0} a_{k_1}^{(1)} a_{-k_1}^{(2)} + a_0^{(1)} a_0^{(2)} + \sum_{k_1>0} a_{k_1}^{(1)} a_{-k_1}^{(2)} \\ &= a_0^{(1)} a_0^{(2)} + 2 \sum_{k_1=1}^{\infty} a_{k_1}^{(1)} a_{k_1}^{(2)} \\ &\in A_1 A_2 \left[1 + 2 \sum_{k_1=1}^{\infty} \frac{1}{k_1^{2s}} \right] [-1,1] \\ &\subseteq A_1 A_2 \left[4 + \frac{1}{2^{2s-1}(2s-1)} \right] [-1,1] \\ &= \alpha_0^{(2)} A_1 A_2 \, [-1,1] \, . \end{aligned}$$

Now consider $k \in \{1, \ldots, M-1\}$. Then

$$\begin{aligned} \sum_{\substack{k_1+k_2=k \\ k_i \in \mathbb{Z}}} a_{k_1}^{(1)} a_{k_2}^{(2)} &= \sum_{k_1=-\infty}^{-1} a_{k_1}^{(1)} a_{k-k_1}^{(2)} + a_0^{(1)} a_k^{(2)} + \sum_{k_1=1}^{k-1} a_{k_1}^{(1)} a_{k-k_1}^{(2)} + a_k^{(1)} a_0^{(2)} + \sum_{k_1=k+1}^{\infty} a_{k_1}^{(1)} a_{k-k_1}^{(2)} \\ &\in A_1 A_2 \left[\frac{2}{k^s} + 2 \sum_{k_1=1}^{\infty} \frac{1}{k_1^s (k+k_1)^s} + \frac{1}{k^s} \sum_{k_1=1}^{k-1} \frac{k^s}{k_1^s (k-k_1)^s} \right] [-1,1] \\ &\subset A_1 A_2 \left[\frac{2}{k^s} + \frac{2}{k^s} \sum_{k_1=1}^{\infty} \frac{1}{k_1^s} + \frac{1}{k^s} \sum_{k_1=1}^{k-1} \frac{k^s}{k_1^s (k-k_1)^s} \right] [-1,1] \\ &\subseteq \frac{\alpha_k^{(2)} A_1 A_2}{k^s} \, [-1,1] \, , \end{aligned}$$

where we, quite arbitrarily, have bound the infinite sum $\sum_{k_1=1}^{\infty} \frac{1}{k_1^s}$ using an integral estimate after the third term. For the case $k \geq M$, we do the same analysis than in the case $k \in \{1, \ldots, M-1\}$ and we use the upper bound γ_k from Lemma 24. □

Remark 26. *For any $k \geq M \geq 6$, we have that $\alpha_k^{(2)} \leq \alpha_M^{(2)}$.*

Proof. For $k \geq 6$, the fact that $\frac{\ln(k-1)}{(k+1)} \leq \frac{\ln(k-2)}{k}$ implies that $\gamma_{k+1}^{(s)} \leq \gamma_k^{(s)}$. The conclusion then follows from the definition $\alpha_k^{(2)}$ for $k \geq M \geq 6$. □

A.2 Estimates for a general nonlinearity

Let $p \geq 3$ be the degree of the nonlinearity, $s \geq 2$ the decay of the coefficients, and $M \geq 6$ a natural number. We compute the general estimates recursively. Hence, we

first suppose that for every $k \geq 0$, we know explicitly $\alpha_k^{(p-1)} > 0$ such that

$$\sum_{\substack{k_1+\cdots+k_{p-1}=k \\ k_i\in\mathbb{Z}}} a_{k_1}^{(1)} \cdots a_{k_{p-1}}^{(p-1)} \in \begin{cases} \alpha_0^{(p-1)} \left(\prod_{i=1}^{p-1} A_i\right) [-1,1] & k=0, \\ \frac{\alpha_k^{(p-1)}}{|k|^s} \left(\prod_{i=1}^{p-1} A_i\right) [-1,1] & k \neq 0. \end{cases}$$

and such that $\alpha_k^{(p-1)} \leq \alpha_M^{(p-1)}$ for all $k \geq M$. We define

$$\alpha_k^{(p)} \stackrel{\text{def}}{=} \begin{cases} \alpha_0^{(p-1)} + 2\sum_{k_p=1}^{M-1} \frac{\alpha_{k_p}^{(p-1)}}{k_p^{2s}} + \frac{2\alpha_M^{(p-1)}}{(M-1)^{2s-1}(2s-1)}, & \text{for } k=0; \\ \sum_{k_p=1}^{M-k-1} \frac{\alpha_{k+k_p}^{(p-1)} k^s}{k_p^s (k+k_p)^s} + \alpha_M^{(p-1)} \left(1 + \frac{1}{2^s} + \frac{1}{3^s} + \frac{1}{3^{s-1}(s-1)}\right) & \\ \quad + \alpha_k^{(p-1)} + \sum_{k_p=1}^{k-1} \frac{\alpha_{k_p}^{(p-1)} k^s}{k_p^s (k-k_p)^s} + \alpha_0^{(p-1)} + \sum_{k_p=1}^{M-1} \frac{\alpha_{k_p}^{(p-1)} k^s}{(k+k_p)^s k_p^s} & \\ \quad + \frac{\alpha_M^{(p-1)}}{(M-1)^{s-1}(s-1)}, & \text{for } 1 \leq k \leq M-1; \\ \alpha_M^{(p-1)} \left[2 + \frac{1}{2^s} + \frac{1}{3^s} + \frac{1}{3^{s-1}(s-1)} + \frac{1}{(M-1)^{s-1}(s-1)} + \gamma_k\right] & \\ \quad + \alpha_0^{(p-1)} + \sum_{k_p=1}^{M-1} \frac{\alpha_{k_p}^{(p-1)}}{k_p^s} \left[1 + \frac{1}{\left[1-\frac{k_p}{M}\right]^s}\right], & \text{for } k \geq M. \end{cases}$$

Lemma 27. *For $i = 1, \ldots, p$, let $A_i > 0$ such that $a_0^{(i)} \in A_i[-1,1]$ and $a_k^{(i)} \in \frac{A_i}{|k|^s}[-1,1]$, for all $k \neq 0$. Suppose that $a_{-k}^{(i)} = a_k^{(i)}$. Then*

$$\sum_{\substack{k_1+\cdots+k_p=k \\ k_i\in\mathbb{Z}}} a_{k_1}^{(1)} \cdots a_{k_p}^{(p)} \in \begin{cases} \alpha_0^{(p)} \left(\prod_{i=1}^{p} A_i\right) [-1,1] & k=0, \\ \frac{\alpha_k^{(p)}}{|k|^s} \left(\prod_{i=1}^{p} A_i\right) [-1,1] & k \neq 0. \end{cases}$$

Proof. Throughout the proof, we use several times that $\alpha_k^{(p-1)} \leq \alpha_M^{(p-1)}$ for all $k \geq M$. For $k=0$,

$$\begin{aligned} \sum_{\substack{k_1+\cdots+k_p=0 \\ k_i\in\mathbb{Z}}} a_{k_1}^{(1)} \cdots a_{k_p}^{(p)} &= \sum_{k_p=-\infty}^{-1} a_{k_p}^{(p)} \sum_{\substack{k_1+\cdots+k_{p-1}=-k_p \\ k_i\in\mathbb{Z}}} a_{k_1}^{(1)} \cdots a_{k_{p-1}}^{(p-1)} \\ &\quad + a_0^{(p)} \sum_{\substack{k_1+\cdots+k_{p-1}=0 \\ k_i\in\mathbb{Z}}} a_{k_1}^{(1)} \cdots a_{k_{p-1}}^{(p-1)} \\ &\quad + \sum_{k_p=1}^{\infty} a_{k_p}^{(p)} \sum_{\substack{k_1+\cdots+k_{p-1}=-k_p \\ k_i\in\mathbb{Z}}} a_{k_1}^{(1)} \cdots a_{k_{p-1}}^{(p-1)} \\ &\in \left(\prod_{i=1}^{p} A_i\right) \left[\sum_{k_p=1}^{\infty} \frac{\alpha_{k_p}^{(p-1)}}{k_p^{2s}} + \alpha_0^{(p-1)} + \sum_{k_p=1}^{\infty} \frac{\alpha_{k_p}^{(p-1)}}{k_p^{2s}}\right] [-1,1] \\ &\subseteq \left(\prod_{i=1}^{p} A_i\right) \left[\alpha_0^{(p-1)} + 2\sum_{k_p=1}^{M-1} \frac{\alpha_{k_p}^{(p-1)}}{k_p^{2s}} + \frac{2\alpha_M^{(p-1)}}{(M-1)^{2s-1}(2s-1)}\right] [-1,1] \\ &= \alpha_0^{(p)} \left(\prod_{i=1}^{p} A_i\right) [-1,1]. \end{aligned}$$

For any $k \geq 1$,

$$\begin{aligned}
\sum_{\substack{k_1+\cdots+k_p=k\\ k_i\in\mathbb{Z}}} a_{k_1}^{(1)}\cdots a_{k_p}^{(p)} &= \sum_{k_p=-\infty}^{-1} a_{k_p}^{(p)} \sum_{\substack{k_1+\cdots+k_{p-1}=k-k_p\\ k_i\in\mathbb{Z}}} a_{k_1}^{(1)}\cdots a_{k_{p-1}}^{(p-1)} \\
&\quad + a_0^{(p)} \sum_{\substack{k_1+\cdots+k_{p-1}=k\\ k_i\in\mathbb{Z}}} a_{k_1}^{(1)}\cdots a_{k_{p-1}}^{(p-1)} + \sum_{k_p=1}^{k-1} a_{k_p}^{(p)} \sum_{\substack{k_1+\cdots+k_{p-1}=k-k_p\\ k_i\in\mathbb{Z}}} a_{k_1}^{(1)}\cdots a_{k_{p-1}}^{(p-1)} \\
&\quad + a_k^{(p)} \sum_{\substack{k_1+\cdots+k_{p-1}=0\\ k_i\in\mathbb{Z}}} a_{k_1}^{(1)}\cdots a_{k_{p-1}}^{(p-1)} + \sum_{k_p=k+1}^{\infty} a_{k_p}^{(p)} \sum_{\substack{k_1+\cdots+k_{p-1}=k-k_p\\ k_i\in\mathbb{Z}}} a_{k_1}^{(1)}\cdots a_{k_{p-1}}^{(p-1)} \\
&\in \left(\prod_{i=1}^{p} A_i\right)\left[\sum_{k_p=1}^{\infty}\frac{\alpha_{k+k_p}^{(p-1)}}{k_p^s(k+k_p)^s} + \frac{\alpha_k^{(p-1)}}{k^s} + \sum_{k_p=1}^{k-1}\frac{\alpha_{k_p}^{(p-1)}}{k_p^s(k-k_p)^s}\right. \\
&\qquad \left. + \frac{\alpha_0^{(p-1)}}{k^s} + \sum_{k_p=1}^{\infty}\frac{\alpha_{k_p}^{(p-1)}}{(k+k_p)^s k_p^s}\right][-1,1].
\end{aligned}$$

Consider now $k \in \{1,\ldots,M-1\}$. Since $\alpha_{k_p}^{(p-1)} \leq \alpha_M^{(p-1)}$, for all $k_p \geq M$, we have

$$\begin{aligned}
\sum_{k_p=1}^{\infty}\frac{\alpha_{k+k_p}^{(p-1)}}{k_p^s(k+k_p)^s} &= \sum_{k_p=1}^{M-k-1}\frac{\alpha_{k+k_p}^{(p-1)}}{k_p^s(k+k_p)^s} + \sum_{k_p=M-k}^{\infty}\frac{\alpha_{k+k_p}^{(p-1)}}{k_p^s(k+k_p)^s} \\
&\leq \sum_{k_p=1}^{M-k-1}\frac{\alpha_{k+k_p}^{(p-1)}}{k_p^s(k+k_p)^s} + \alpha_M^{(p-1)}\sum_{k_p=M-k}^{\infty}\frac{1}{k_p^s(k+k_p)^s} \\
&\leq \sum_{k_p=1}^{M-k-1}\frac{\alpha_{k+k_p}^{(p-1)}}{k_p^s(k+k_p)^s} + \alpha_M^{(p-1)}\sum_{k_p=1}^{\infty}\frac{1}{k_p^s(k+k_p)^s} \\
&\leq \frac{1}{k^s}\left[\sum_{k_p=1}^{M-k-1}\frac{\alpha_{k+k_p}^{(p-1)}k^s}{k_p^s(k+k_p)^s} + \alpha_M^{(p-1)}\left(1+\frac{1}{2^s}+\frac{1}{3^s}+\frac{1}{3^{s-1}(s-1)}\right)\right].
\end{aligned}$$

Similarly,

$$\sum_{k_p=1}^{\infty}\frac{\alpha_{k_p}^{(p-1)}}{(k+k_p)^s k_p^s} \leq \frac{1}{k^s}\left[\sum_{k_p=1}^{M-1}\frac{\alpha_{k_p}^{(p-1)}k^s}{(k+k_p)^s k_p^s} + \frac{\alpha_M^{(p-1)}}{(M-1)^{s-1}(s-1)}\right].$$

Recalling the definition of $\alpha_k^{(p)}$ for the cases $k \in \{1,\ldots,M-1\}$, we get that

$$\sum_{\substack{k_1+\cdots+k_p=k\\ k_i\in\mathbb{Z}}} a_{k_1}^{(1)}\cdots a_{k_p}^{(p)} \in \frac{\alpha_k^{(p)}}{k^s}\left(\prod_{i=1}^{p} A_i\right)[-1,1].$$

Consider now $k \geq M$, then

$$\sum_{k_p=1}^{\infty}\frac{\alpha_{k+k_p}^{(p-1)}}{k_p^s(k+k_p)^s} + \frac{\alpha_k^{(p-1)}}{k^s} \leq \frac{\alpha_M^{(p-1)}}{k^s}\left[2+\frac{1}{2^s}+\frac{1}{3^s}+\frac{1}{3^{s-1}(s-1)}\right].$$

Using Lemma 24, we get that

$$\begin{aligned}\sum_{k_p=1}^{k-1}\frac{\alpha_{k_p}^{(p-1)}}{k_p^s(k-k_p)^s} &= \sum_{k_p=1}^{M-1}\frac{\alpha_{k_p}^{(p-1)}}{k_p^s(k-k_p)^s}+\frac{1}{k^s}\sum_{k_p=M}^{k-1}\frac{k^s\alpha_{k_p}^{(p-1)}}{k_p^s(k-k_p)^s}\\ &\le \frac{1}{k^s}\sum_{k_p=1}^{M-1}\frac{\alpha_{k_p}^{(p-1)}}{k_p^s\left(1-\frac{k_p}{k}\right)^s}+\frac{\alpha_M^{(p-1)}}{k^s}\sum_{k_p=M}^{k-1}\frac{k^s}{k_p^s(k-k_p)^s}\\ &\le \frac{1}{k^s}\left[\sum_{k_p=1}^{M-1}\frac{\alpha_{k_p}^{(p-1)}}{k_p^s\left(1-\frac{k_p}{M}\right)^s}+\alpha_M^{(p-1)}\gamma_k\right].\end{aligned}$$

Also,

$$\sum_{k_p=1}^{\infty}\frac{\alpha_{k_p}^{(p-1)}}{(k+k_p)^s k_p^s}\le\frac{1}{k^s}\left[\sum_{k_p=1}^{M-1}\frac{\alpha_{k_p}^{(p-1)}}{k_p^s}+\frac{\alpha_M^{(p-1)}}{(M-1)^{s-1}(s-1)}\right].$$

Combining the three above inequalities, we finally have that

$$\begin{aligned}&\sum_{\substack{k_1+\cdots+k_p=k\\ k_i\in\mathbb{Z}}} a_{k_1}^{(1)}\cdots a_{k_p}^{(p)}\\ &\quad\in\frac{1}{k^s}\left(\prod_{i=1}^{p}A_i\right)\left[\alpha_0^{(p-1)}+\sum_{k_p=1}^{M-1}\frac{\alpha_{k_p}^{(p-1)}}{k_p^s}\left(1+\frac{1}{\left(1-\frac{k_p}{M}\right)^s}\right)\right.\\ &\qquad\left.+\alpha_M^{(p-1)}\left(2+\tfrac{1}{2^s}+\tfrac{1}{3^s}+\tfrac{1}{3^{s-1}(s-1)}+\tfrac{1}{(M-1)^{s-1}(s-1)}+\gamma_k\right)\right][-1,1]\\ &\quad=\frac{\alpha_k^{(p)}}{k^s}\left(\prod_{i=1}^{p}A_i\right)[-1,1].\end{aligned}$$

□

Remark 28. *For any $k\ge M\ge 6$, we have that $\alpha_k^{(p)}\le\alpha_M^{(p)}$.*

Proof. The proof is identical to that of Remark 26. □

A.3 Comparison of the general estimates

We now compare the new estimates with the ones given by Lemma 23 for different values of p and s. Since the only difference in the estimates is α^{p-1} versus $\alpha_k^{(p)}$, these are the quantities we compare in Table 5. In particular, the new estimates lead to an improvement of a factor 10^2 for the values $p=3$ and $s=4$ used in this paper, while for higher values of p and s they become even more beneficial. For the computation, we fixed $M=100$; in the case $p\ge 3$, increasing M would make the $\alpha_k^{(p)}$ smaller still.

A.4 Refinement for $k\in\{0,\dots,M-1\}$

We now present a corollary of Lemma 27, which gives better bounds for $0\le k\le M-1$.

Corollary 29. *Let $p\ge 3$ to be the degree of the nonlinearity, $s\ge 2$ the decay of the coefficients and $M\ge 6$ a natural number. Consider another computational number $M_1\ge M$. Let the $\{\alpha_k^{(p-1)}\}_{k\in\{0,\dots,M_1\}}$ be defined in Lemma 27. For $i=1,\dots,p$, let*

p	s	k	α^{p-1}	$\alpha_k^{(p)}$
2	4	10	$5.87 \cdot 10^1$	$6.65 \cdot 10^0$
3	4	30	$3.44 \cdot 10^3$	$4.44 \cdot 10^1$
3	4	90	$3.44 \cdot 10^3$	$4.31 \cdot 10^1$
3	5	30	$1.31 \cdot 10^4$	$4.20 \cdot 10^1$
3	7	30	$2.03 \cdot 10^5$	$4.12 \cdot 10^1$
3	10	30	$1.29 \cdot 10^7$	$4.26 \cdot 10^1$
3	50	30	$1.55 \cdot 10^{31}$	$1.68 \cdot 10^2$
4	4	10	$2.02 \cdot 10^5$	$3.28 \cdot 10^2$
4	5	10	$1.50 \cdot 10^6$	$3.17 \cdot 10^2$
4	7	10	$9.13 \cdot 10^7$	$3.59 \cdot 10^2$
5	10	10	$1.65 \cdot 10^{14}$	$3.98 \cdot 10^3$
5	20	10	$1.81 \cdot 10^{26}$	$1.82 \cdot 10^5$
10	25	20	$4.25 \cdot 10^{72}$	$1.75 \cdot 10^8$
20	50	90	$2.07 \cdot 10^{296}$	$5.01 \cdot 10^{15}$

Table 5: Comparison of the estimates α^{p-1} versus $\alpha_k^{(p)}$ used in Lemmas 23 and 27.

$A_i > 0$ be such that $a_0^{(i)} \in A_i[-1,1]$ and $a_k^{(i)} \in \frac{A_i}{|k|^s}[-1,1]$, for all $k \neq 0$, and let $|a|_{M_1}^{(i)} = \left(|a_0^{(i)}|, \ldots, |a_{M_1-1}^{(i)}|\right)$. Suppose that $a_{-k}^{(i)} = a_k^{(i)}$. For $k \in \{0, \ldots, M-1\}$, define

$$\varepsilon_k^{(p)} = \frac{2\alpha_{M_1}^{(p-1)}}{(M_1+k)^s (M_1-1)^{s-1}(s-1)} + \sum_{k_p=M_1}^{M_1+k-1} \frac{\alpha_{k_p-k}^{(p-1)}}{k_p^s (k_p-k)^s}\,.$$

Then we have that, for $k \in \{0, \ldots, M-1\}$,

$$\left(a^{(1)} * \cdots * a^{(p)}\right)_k \in \left[\left(|a|_{M_1}^{(1)} * \cdots * |a|_{M_1}^{(p)}\right)_k + \left(\prod_{i=1}^{p} A_i\right) \varepsilon_k^{(p)}\right][-1,1]\,.$$

Proof. First notice that

$$\begin{aligned}\left(a^{(1)} * \cdots * a^{(p)}\right)_k &= \sum_{\substack{k_1+\cdots+k_p=k \\ k_i \in \mathbb{Z}}} a_{k_1}^{(1)} \cdots a_{k_p}^{(p)} \\ &= \sum_{\substack{k_1+\cdots+k_p=k \\ |k_i|<M_1}} a_{k_1}^{(1)} \cdots a_{k_p}^{(p)} + \sum_{\substack{k_1+\cdots+k_p=k \\ \max\{|k_1|,\cdots,|k_p|\} \geq M_1}} a_{k_1}^{(1)} \cdots a_{k_p}^{(p)}\,.\end{aligned}$$

Without loss of generality, suppose that $|k_p| \geq M_1$ in the second sum. Then

$$\begin{aligned}
\sum_{\substack{k_1+\cdots+k_p=k \\ \max\{|k_i|\}\geq M_1}} a_{k_1}^{(1)} \cdots a_{k_p}^{(p)} &= \sum_{k_p=-\infty}^{-M_1} a_{k_p}^{(p)} \sum_{k_1+\cdots+k_{p-1}=k-k_p} a_{k_1}^{(1)} \cdots a_{k_{p-1}}^{(p-1)} \\
&\quad + \sum_{k_p=M_1}^{\infty} a_{k_p}^{(p)} \sum_{k_1+\cdots+k_{p-1}=k-k_p} a_{k_1}^{(1)} \cdots a_{k_{p-1}}^{(p-1)} \\
&\in \left(\prod_{i=1}^{p} A_i\right) \sum_{k_p=M_1}^{\infty} \left[\frac{\alpha_{k+k_p}^{(p-1)}}{k_p^s(k+k_p)^s} + \frac{\alpha_{k_p-k}^{(p-1)}}{k_p^s(k_p-k)^s}\right][-1,1] \\
&\subseteq \left(\prod_{i=1}^{p} A_i\right) \left[2\alpha_{M_1}^{(p-1)} \sum_{k_p=M_1}^{\infty} \frac{1}{k_p^s(k+k_p)^s} + \sum_{k_p=M_1}^{M_1+k-1} \frac{\alpha_{k_p-k}^{(p-1)}}{k_p^s(k_p-k)^s}\right][-1,1] \\
&\subseteq \left(\prod_{i=1}^{p} A_i\right) \left[\frac{2\alpha_{M_1}^{(p-1)}}{(M_1+k)^s(M_1-1)^{s-1}(s-1)} + \sum_{k_p=M_1}^{M_1+k-1} \frac{\alpha_{k_p-k}^{(p-1)}}{k_p^s(k_p-k)^s}\right][-1,1].
\end{aligned}$$

Recalling the definition of $\varepsilon_k^{(p)}$, we can conclude that

$$\left(a^{(1)} * \cdots * a^{(p)}\right)_k \in \left[\left(|a|_{M_1}^{(1)} * \cdots * |a|_{M_1}^{(p)}\right)_k + \left(\prod_{i=1}^{p} A_i\right) \varepsilon_k^{(p)}\right][-1,1]. \qquad \square$$

References

[1] G. Arioli and P. Zgliczyński, *Symbolic dynamics for the Hénon-Heiles Hamiltonian on the critical level*, J. Differential Equations, 171 (2001), pp. 173–202.

[2] J. B. van den Berg, L. A. Peletier, and W. C. Troy, *Global branches of multi-bump periodic solutions of the Swift-Hohenberg equation*, Arch. Ration. Mech. Anal., 158 (2001), pp. 91–153.

[3] J. B. van den Berg and R. C. Vandervorst, *Second order Lagrangian twist systems: simple closed characteristics*, Trans. Amer. Math. Soc., 354 (2002), pp. 1393–1420 (electronic).

[4] ——, *Stable patterns for fourth-order parabolic equations*, Duke Math. J., 115 (2002), pp. 513–558.

[5] J.B. van den Berg, J.-P. Lessard, and K. Mischaikow, *Rigorous branch following*, 2008. In preparation.

[6] B. Buffoni, *Periodic and homoclinic orbits for Lorentz-Lagrangian systems via variational methods*, Nonlinear Anal., 26 (1996), pp. 443–462.

[7] B. Buffoni, A. R. Champneys, and J. F. Toland, *Bifurcation and coalescence of a plethora of homoclinic orbits for a Hamiltonian system*, J. Dynam. Differential Equations, 8 (1996), pp. 221–279.

[8] B. Buffoni and J. F. Toland, *Global existence of homoclinic and periodic orbits for a class of autonomous Hamiltonian systems*, J. Differential Equations, 118 (1995), pp. 104–120.

[9] A. R. Champneys, *Homoclinic orbits in reversible systems and their applications in mechanics, fluids and optics*, Phys. D, 112 (1998), pp. 158–186. Time-reversal symmetry in dynamical systems (Coventry, 1996).

[10] M. C. Cross and P. C. Hohenberg, *Pattern formation outside of equilibrium*, Rev. Mod. Phys., 65 (1993), pp. 851–1112.

[11] S. Day, *A rigorous numerical method in infinite dimensions*, PhD thesis, Georgia Institute of Technology, 2003.

[12] S. Day, Y. Hiraoka, K. Mischaikow, and T. Ogawa, *Rigorous numerics for global dynamics: a study of the Swift-Hohenberg equation*, SIAM J. Appl. Dyn. Syst., 4 (2005), pp. 1–31 (electronic).

[13] S. Day, O. Junge, and K. Mischaikow, *A rigorous numerical method for the global analysis of infinite-dimensional discrete dynamical systems*, SIAM J. Appl. Dyn. Syst., 3 (2004), pp. 117–160 (electronic).

[14] S. Day, J.-P. Lessard, and K. Mischaikow, *Validated continuation for equilibria of PDEs*, SIAM Journal on Numerical Analysis, 45 (2007), pp. 1398–1424.

[15] R. L. Devaney, *Homoclinic orbits in Hamiltonian systems*, J. Differential Equations, 21 (1976), pp. 431–438.

[16] M. Gameiro, T. Gedeon, W. Kalies, H. Kokubu, K. Mischaikow, and H. Oka, *Topological horseshoes of travelling waves for a fast-slow predator-prey system*, J. Dynam. Differential Equations, 19 (2007), pp. 623–654.

[17] M. Gameiro, J.-P. Lessard, and K. Mischaikow, *Validated continuation over large parameter ranges for equilibria of PDEs*, 2007. To appear in Mathematics and Computers in Simulation.

[18] R. W. Ghrist, J. B. van den Berg, and R. C. Vandervorst, *Morse theory on spaces of braids and Lagrangian dynamics*, Invent. Math., 152 (2003), pp. 369–432.

[19] G.I. Hargreaves, *Interval analysis in matlab*, Numerical Analysis Report, University of Manchester, (2002).

[20] W. D. Kalies, J. Kwapisz, J. B. van den Berg, and R. C. A. M. Vander-Vorst, *Homotopy classes for stable periodic and chaotic patterns in fourth-order Hamiltonian systems*, Comm. Math. Phys., 214 (2000), pp. 573–592.

[21] W. D. Kalies, J. Kwapisz, and R. C. A. M. VanderVorst, *Homotopy classes for stable connections between Hamiltonian saddle-focus equilibria*, Comm. Math. Phys., 193 (1998), pp. 337–371.

[22] W. D. Kalies and R. C. A. M. VanderVorst, *Multitransition homoclinic and heteroclinic solutions of the extended Fisher-Kolmogorov equation*, J. Differential Equations, 131 (1996), pp. 209–228.

[23] T. Y. Li and J. A. Yorke, *Period three implies chaos*, Amer. Math. Monthly, 82 (1975), pp. 985–992.

[24] K. Mischaikow and M. Mrozek, *Chaos in the Lorenz equations: a computer-assisted proof*, Bull. Amer. Math. Soc. (N.S.), 32 (1995), pp. 66–72.

[25] L. A. Peletier and W. C. Troy, *Chaotic spatial patterns described by the extended Fisher-Kolmogorov equation*, J. Differential Equations, 129 (1996), pp. 458–508.

[26] ——, *Spatial patterns; higher order models in physics and mechanics*, Progress in Nonlinear Differential Equations and their Applications, 45, Birkhäuser Boston Inc., Boston, MA, 2001.

[27] M. A. Peletier, *Sequential buckling: a variational analysis*, SIAM J. Math. Anal., 32 (2001), pp. 1142–1168 (electronic).

[28] C. Robinson, *Dynamical systems; Stability, symbolic dynamics, and chaos*, Studies in Advanced Mathematics, CRC Press, Boca Raton, FL, second ed., 1999.

[29] J. Swift and P. C. Hohenberg, *Hydrodynamic fluctuations at the convective instability*, Phys. Rev. A, 15 (1977), pp. 319–328.

[30] A. Szymczak, *The Conley index and symbolic dynamics*, Topology, 35 (1996), pp. 287–299.

[31] W. P. Thurston, *On the geometry and dynamics of diffeomorphisms of surfaces*, Bull. Amer. Math. Soc. (N.S.), 19 (1988), pp. 417–431.

[32] W. Tucker, *The Lorenz attractor exists*, C. R. Acad. Sci. Paris Sér. I Math., 328 (1999), pp. 1197–1202.

[33] D. Wilczak, *Chaos in the Kuramoto-Sivashinsky equations—a computer-assisted proof*, J. Differential Equations, 194 (2003), pp. 433–459.

[34] N. Yamamoto, *A numerical verification method for solutions of boundary value problems with local uniqueness by Banach's fixed-point theorem*, SIAM J. Numer. Anal., 35 (1998), pp. 2004–2013 (electronic).

[35] P. Zgliczyński and K. Mischaikow, *Rigorous numerics for partial differential equations: the Kuramoto-Sivashinsky equation*, Found. Comput. Math., 1 (2001), pp. 255–288.